View metadata, citation and similar papers at core.ac.uk
brought to you by CORE
provided by CERN Document Server

Protostellar Collapse with Various Metallicities

Kazuyuki Omukai
Department of Physics, Kyoto University, Kyoto 606-8502, Japan

ABSTRACT

The thermal and chemical evolution of gravitationally collapsing protostellar clouds is investigated, focusing attention on their dependence on metallicity. Calculations are carried out for a range of metallicities spanning the local interstellar value to zero. During the time when clouds are transparent to continuous radiation, the temperatures are higher for those with lower metallicity, reflecting lower radiative ability. However, once the clouds become opaque, in the course of the adiabatic contraction of the transient cores, their evolutionary trajectories in the density-temperature plane converge to a unique curve that is determined by only physical constants. The trajectories coincide with each other thereafter. Consequently, the size of the stellar core at the formation is the same regardless of the gas composition of the parent cloud.

Subject headings: ISM: clouds — ISM: molecules — molecular processes — stars: formation — stars: Population II

1. Introduction

In the standard theory of cosmic structure formation, galaxies are believed to have originated from primeval density fluctuations. Many authors have been studying the galaxy formation process in this context and have made remarkable progress in understanding such processes as the gravitational growth of the density fluctuation, its decoupling from the cosmic expansion and virialization, and the subsequent radiative cooling of the baryonic gas (e.g., Padmanabhan 1993). However, processes after the cooling of baryonic gas, namely, the transformation of a pregalactic cloud into a cluster of stars, are relatively poorly known. It is inevitably necessary to investigate them in studying the galaxy formation process since the very existence of stellar components is one distinct feature of galaxies. These processes can be viewed as successive fragmentations of a cloud into fragments, or in other words, protostellar clouds, and their contraction into stars (e.g., Hayashi 1984).

Whether a cloud fragments or collapses into a single object depends on the the central flatness, that is, the axial ratio of the isodensity contour in the central region (Tsuribe & Inutsuka 1999). In particular, warm clouds do not fragment before adiabatic core formation, whereas clumps sufficiently more massive than the Jeans mass first collapse disklike and next fragment most likely into filamentary clouds (Miyama, Narita, & Hayashi 1987a, 1987b). The filamentary clouds fragment again into protostellar cloud cores after further contraction. Uehara et al. (1997) investigated the gravitational collapse of metal-free filamentary clouds using one-zone approximation and found that the minimum mass of fragments, or protostellar cores, is essentially Chandrasekhar mass, i.e., $\sim 1 M_{\odot}$. Nakamura & Umemura (1999) confirmed Uehara et al. (1997)'s result by performing one-dimensional hydrodynamical calculations. In this paper, we will discuss the collapse of protostellar cores into stars.

The distinction between the star formation in the galaxy formation epoch and that in present-day star-forming regions mainly resides in the difference of the composition of gas that stars are made from. Metallicity, and therefore the gas to dust ratio, is lower for earlier star formation. In present-day star forming regions, protostellar clouds remain roughly 10K in a wide range of densities owing to efficient dust emission (e.g., Hayashi & Nakano 1965) in the course of contraction.

On the other hand, many authors have studied the thermal and chemical evolution of collapsing primordial clouds with one-zone approximation (e.g., Matsuda, Sato, & Takeda 1969; Yoneyama 1972; Calberg 1981; Palla, Salpeter, & Stahler 1983; Izotov & Kolesnik 1984; Lahav 1986; Puy & Signore 1997) or by hydrodynamical calculations (Matsuda et al. 1969; Villere & Bodenheimer 1987; Haiman, Thoul, & Loeb 1996; Omukai & Nishi 1998; Oliveira et al. 1998). The collapse of metal-free protostellar clouds, which is relevant for the first star formation in the universe, is induced by radiative cooling owing to molecular hydrogen lines, and their temperatures are about 1000K.

Above are two extremes in composition of protostellar gas, namely, the former for the high-metallicity end and the latter for the low-metallicity end.

Then, how does the collapse of slightly metal-polluted clouds proceed? Even in the galaxy formation epoch, significant metal enrichment can occur since the lifetime of massive stars ($\sim 10^6$ yr) is shorter than the free-fall time of pregalactic clouds ($\sim 10^8$ yr). In fact, both Lyα forest clouds and Population II stars are slightly polluted by heavy elements. Therefore, it is important to study star formation from slightly metal-polluted gas. In this paper, we aim to fill the gap between the protostellar collapse of primordial and present-day interstellar gas.

This topic has been investigated in the pioneering works of Low & Lynden-Bell (1976) and Yoshii &

Sabano (1980). However, the following points remain to be fulfilled; in their works, (i) chemical reactions had not been solved, (ii) molecular coolants, which become important at high densities, had not been considered, and (iii) the evolution of clouds as dense as the stellar density ($> 10^{22}\mathrm{cm}^{-3}$) had not been studied. With these points in mind, we investigate in this paper the thermal and chemical evolution of collapsing spherical clouds as a function of metallicity.

The outline of this paper is as follows. In §2, we describe the method of our calculations. In §3, results of our calculations are presented. We summarize our work in §4.

2. Model

2.1. Basic Equations

We consider a spherical cloud with mean metallicity Z. The helium concentration is assumed to be $y_{\mathrm{He}} = 0.0972$ for all clouds.[1] We assume that the dust-to-gas ratio is proportional to the mean metallicity, or in other words, that a fixed fraction of the heavy elements in the interstellar medium condenses into dust grains. We adopt the Pollack et al. (1994) model of grains in molecular clouds (see §2.2.2). For the case of local interstellar clouds ($Z \simeq 1Z_{\odot}$), the mass fraction of grain we used is 0.934×10^{-2} in the lowest temperature regime, and the gas-phase elemental abundances are $y_{\mathrm{C}} = 0.927 \times 10^{-4}$, and $y_{\mathrm{O}} = 3.568 \times 10^{-4}$, respectively, which correspond to 46% of oxygen and 72% of carbon depleted onto grains. These values are reduced proportionally for lower metallicity cases. We normalize the mean metallicity (and therefore also the dust-to-gas ratio and gas-phase metallicity in our model) relative to the local interstellar values Z_{local} and denote relative metallicity by $z \equiv Z/Z_{\mathrm{local}}$.

We calculate the time evolution of the central density, temperature, and chemical composition of the collapsing core.

First, we assume that the dynamics is described by the free-fall relation,

$$\frac{d\rho}{dt} = \frac{\rho}{t_{\mathrm{ff}}}, \tag{3}$$

where ρ is the density in the central region and the free-fall time is

$$t_{\mathrm{ff}} \equiv \sqrt{\frac{3\pi}{32G\rho}}. \tag{4}$$

The thermal evolution is followed by solving the energy equation

$$\frac{de}{dt} = -p\frac{d}{dt}(\frac{1}{\rho}) - \mathcal{L}^{(\mathrm{net})}, \tag{5}$$

[1]The concentration of element X is defined by

$$y_X = n_X/n, \tag{1}$$

where n and n_X are the number densities of hydrogen nuclei and nuclei of element X. Similarly, we write for each atomic, molecular, or ionic species

$$y(x) = n(x)/n, \tag{2}$$

where $n(x)$ is the number density of species x. Note $y(\mathrm{H}_2) = 1/2$ for fully molecular gas.

where

$$e = \frac{1}{\gamma_{\rm ad} - 1} \frac{kT}{\mu m_{\rm H}} \tag{6}$$

is the specific internal energy,

$$p = \frac{\rho kT}{\mu m_{\rm H}} \tag{7}$$

is the pressure for an ideal gas, $\gamma_{\rm ad}$ is the adiabatic exponent, T is the temperature, μ is the mean molecular weight, $m_{\rm H}$ is the mass of hydrogen nucleus, and $\mathcal{L}^{(\rm net)}$ is the net energy loss rate per unit mass (see §2.2).

We neglect any effect owing to rotation or magnetic fields for simplicity. In this case, the actual collapse is expected to proceed like the Penston-Larson similarity solution (Penston 1969; Larson 1969). According to this solution, the cloud consists of two parts, that is, the central core region, which has flat density distribution, and the envelope, where the density decreases outward as $\propto r^{-2}$. The size of the central flat region is roughly given by the local Jeans length $\lambda_{\rm J} = \pi c_{\rm s}/\sqrt{G\rho}$ in the core. Since we focus on the evolution of the central region, optical depth is estimated by that across one local Jeans length:

$$\tau_\nu = \kappa_\nu \rho \lambda_{\rm J}. \tag{8}$$

This formulation of Jeans length shielding is the same procedure as that of Low & Lynden-Bell (1976) and Silk (1977), although they introduced it as a result of successive fragmentation into Jeans mass clouds, not because of the Penston-Larson collapse.

2.2. Cooling/Heating processes

In addition to compressional heating, we include cooling owing to (i) atomic and molecular line radiation, (ii) energy transfer between the gas and the dust grains, which will be emitted as infrared radiation from the grains, (iii) continuous radiation from the gas, and (iv) cooling and heating associated with chemical reactions. Then

$$\mathcal{L}^{(\rm net)} = \mathcal{L}_{\rm line} + \mathcal{L}_{\rm gr} + \mathcal{L}_{\rm cont} + \mathcal{L}_{\rm chem}, \tag{9}$$

where the terms in the right-hand side of the equation correspond to the cooling rates owing to the processes (i)-(iv) above in the same order. Although we treat clouds with metallicity up to $\simeq 1 Z_\odot$, we are concerned mainly with the lower metallicity environments that are relevant to the epoch of galaxy formation. In this paper, we do not try to reproduce the present Galactic environment and neglect any external radiation (e.g., UV radiation, cosmic rays, cosmic background radiation, etc.) for simplicity. Then, the considered heating sources are the compressional work and H_2 formation. As will be mentioned below, lower metallicity clouds tend to be warmer. Therefore, the compressional heating, which is proportional to the temperature of the cloud, becomes more important if the external heating rate is constant.

2.2.1. Line Cooling

As line cooling agents, we include atomic fine-structure transitions of CI, CII, and OI and molecular rovibrational transitions of H_2, CO, OH, and H_2O:

$$\mathcal{L}_{\rm line} = \mathcal{L}_{\rm CI} + \mathcal{L}_{\rm CII} + \mathcal{L}_{\rm OI} + \mathcal{L}_{\rm H_2} + \mathcal{L}_{\rm CO} + \mathcal{L}_{\rm OH} + \mathcal{L}_{\rm H_2O}. \tag{10}$$

The line cooling rate of species x is given by

$$\mathcal{L}_x = \frac{1}{\rho} \sum_{(i \to j)} n(x,i) A_{ij} \epsilon_{ij} h\nu_{ij}, \tag{11}$$

where $n(x,i)$ is the population density of species x in level i, A_{ij} is the spontaneous transition probability, ϵ_{ij} is the escape probability, and $h\nu_{ij}$ is the energy difference between levels i and j. The population density $n(x,i)$ is obtained from a solution of the equation of statistical equilibrium

$$n(x,i) \sum_{j \neq i}^{n} R_{ij} = \sum_{j \neq i}^{n} n(x,j) R_{ji}, \tag{12}$$

where n is the total number of lines included and

$$R_{ij} = \begin{cases} A_{ij}\epsilon_{ij} + C_{ij} & \text{for } i > j \\ C_{ij} & \text{for } i < j, \end{cases} \tag{13}$$

ignoring the external radiation. Here C_{ij} is the collisional rate from level i to level j. Following Takahashi, Hollenbach, & Silk (1983), we use the escape probability for the case that the velocity is proportional to the radius in the central region:

$$\epsilon_{ij} = \left(\frac{1 - \mathrm{e}^{-\tau_{ij}}}{\tau_{ij}} \right) \mathrm{e}^{-\tau_{\rm cont}}. \tag{14}$$

The optical depth averaged over the line and the continuum optical depth are given by

$$\tau_{ij} = \frac{A_{ij} c^3}{8\pi \nu_{ij}^3 \eta_{\rm T}} [n(x,j) g_i / g_j - n(x,i)] l_{\rm sh} / (2\Delta v_{\rm D}), \tag{15}$$

and

$$\tau_{\rm cont} = (\kappa_{\rm gr} + \kappa_{\rm gas}) \rho \lambda_{\rm J}, \tag{16}$$

respectively, where $\eta_{\rm T}$ is the multiplicity factor, g_i is the statistical weight of level i, $\Delta v_{\rm D}$ is the velocity dispersion, and $l_{\rm sh}$ is the shielding length (Takahashi et al. 1983):

$$l_{\rm sh} = \min(\Delta s_{\rm th}, \lambda_{\rm J}); \qquad \Delta s_{\rm th} = 2\Delta v_{\rm D} / (\frac{dv}{dr}) = 6 \Delta v_{\rm D} t_{\rm ff}, \tag{17}$$

where we have used the relation for the homogeneous collapse $v = r/3t_{\rm ff}$ and, in the case of the small velocity gradient, have assumed Jeans length shielding as introduced in §2. As a source of the velocity dispersion, we consider only the thermal motion of atoms and neglect microturbulent motions. Then

$$\Delta v_{\rm D} = \sqrt{\frac{2kT}{\mu_x m_{\rm H}}}, \tag{18}$$

where μ_x is the molecular weight of species x. The continuum Planck mean opacity of dust $\kappa_{\rm gr}$ and that of gas $\kappa_{\rm gas}$ are adopted from Pollack et al.(1994) and Lenzuni, Chernoff, & Salpeter (1991), respectively (see §2.2.2 and 2.2.3).

In general, the level population and the escape probabilities depend on each other. We then need an iterative procedure to find their consistent solution except for the case of H_2. For H_2 lines, we need not iterate to find the consistent set of the level populations and the escape probabilities, since in our

calculations, clouds become opaque to H_2 lines only at the density exceeding the critical density, and in such a case, molecules populate following a Boltzmann distribution regardless of the escape probabilities.

The related parameters of transitions are given in Hollenbach & McKee (1989) for CI, CII, and OI, in Hollenbach & McKee (1979;1989) for OH and H_2O [2], and in McKee et al. (1982) for CO. We computed the population of H_2 following the procedure of Hollenbach & McKee (1979) using the collision coefficient given in Hollenbach & McKee (1989). For H_2, we considered the first three vibrational states ($v = 0 - 2$) with rotational levels up to $J = 20$ in each vibrational state. We take into account only the ground vibrational level for other molecular lines since cooling rates owing to vibrational transitions are nearly always dominated by grain cooling or H_2 cooling (Hollenbach & McKee 1979).

2.2.2. Gas-Grain Heat Transfer

We adopt the Pollack et al. (1994) model of grains in molecular clouds. In their model, silicates, organics, troilite, metallic iron, and water ice constitute the most abundant grain species and the dominant sources of opacity in molecular cloud cores. The Planck mean opacity due to the grains in the case of mean metallicity $Z = Z_{\rm local}$ is

$$\kappa_{\rm gr} = 4.0 \times 10^{-4} T_{\rm gr}^2 \ {\rm cm}^2 \ {\rm g}^{-1}, \tag{19}$$

in $T_{\rm gr} \lesssim 50$K, where $T_{\rm gr}$ is the effective grain temperature (see below). The mass fraction of grain is 0.934×10^{-2} below the water vaporization temperature (100-200 K, depending on the density), and that of each component; water ice, volatile organics, refractory organics, troilite, orthopyroxene, olivine and metallic iron are $1.19 \times 10^{-3}, 6.02 \times 10^{-4}, 3.53 \times 10^{-3}, 5.69 \times 10^{-4}, 7.33 \times 10^{-4}, 2.51 \times 10^{-3}$, and 2.53×10^{-4}, respectively (from Table 2 of Pollack et al. 1994). For the grain size distribution

$$n(a) \propto \begin{cases} a^{-3.5} & (0.005\mu{\rm m} < a < 1\mu{\rm m}) \\ a^{-5.5} & (1\mu{\rm m} < a < 5\mu{\rm m}) \end{cases} \tag{20}$$

(Pollack et al. 1994) that is based on that derived by Mathis, Rumpl, & Nordsieck (1977), the energy transfer rate from the gas to the dust grains per unit mass is given by

$$\mathcal{L}_{\rm gr} = 1.1 \times 10^5 n (\frac{f_{\rm gr}}{\rho_{\rm gr}}) (\frac{T}{1000{\rm K}})^{1/2} [1 - 0.8{\rm exp}(-75{\rm K}/T)](T - T_{\rm gr}) \tag{21}$$

(Hollenbach & McKee 1979), where $T_{\rm gr}$ is an effective grain temperature, which is determined by the energy balance for dust grains;

$$\mathcal{L}_{\rm gr} = 4\sigma T_{\rm gr}^4 \kappa_{\rm gr} \beta_{\rm cont}, \tag{22}$$

where $\kappa_{\rm gr}$ is the Planck mean opacity owing to the dust grains and $f_{\rm gr}/\rho_{\rm gr}$ is the total volume of dust grains per unit mass of gas and $f_{\rm gr}/\rho_{\rm gr} = 5.3 \times 10^{-3}$ at the lowest temperatures (i.e., below the water ice vaporization temperature). These quantities are taken from tables in Pollack et al.(1994).

The continuum energy transport rate $\beta_{\rm cont}$ decreases as $\tau_{\rm cont}^{-2}$ owing to radiative diffusion in the optically thick case (e.g., Masunaga et al. 1998). Then,

$$\beta_{\rm cont} = \min(1, \tau_{\rm cont}^{-2}). \tag{23}$$

---

[2]The OH and H_2O collision cross sections and H_2O multiplicity factor are given in Hollenbach & McKee (1989). We adopted other parameters from Hollenbach & McKee (1979).

2.2.3. Continuum of Gas

Using the Planck mean opacity of gas $\kappa_{\rm gas}$, the cooling rate owing to the gas continuum is given by

$$\mathcal{L}_{\rm cont} = 4\sigma T^4 \kappa_{\rm gas} \beta_{\rm cont}. \tag{24}$$

We take the continuum Planck mean opacity for metal-free gas from Lenzuni et al. (1991), which includes all the important continuum processes, specifically, bound-free absorption by H^0 and H^-; free-free absorption by H^0, H^-, H_2, H_2^-, H_2^+, H_3^+, He^0, He^-; photodissociation of H_2, and H_2^+ by thermal radiation; Rayleigh scattering by H^0, H_2, He^0; Thomson scattering by e^-; and collision-induced absorption by H_2 due to collisions with H_2, He^0, and H^0. Among the above processes, the most important cooling mechanism is H_2 collision-induced continuum, which dominates the cooling at about $\sim 10^{16}{\rm cm}^{-3}$ for low metallicity (i.e., $< 10^{-6} Z_\odot$) clouds.

2.2.4. Chemical Cooling/Heating

Following Hollenbach & McKee (1979), we assume the heat deposited per a formed molecular hydrogen as $0.2 + 4.2(1 + n_{\rm cr}/n)^{-1}$ eV for H_2 formation on grain surfaces (reaction 23 in Appendix), $3.53(1 + n_{\rm cr}/n)^{-1}$ eV for H_2 formation by H^- process (reaction 8), $1.83(1 + n_{\rm cr}/n)^{-1}$ eV for H_2 formation by H_2^+ process (reaction 10), and $4.48(1 + n_{\rm cr}/n)^{-1}$ eV for H_2 formation by the three-body reactions (reactions 19 and 20), where

$$n_{\rm cr} = \frac{10^6 T^{-1/2}}{1.6 y({\rm H}) \exp[-(400/T)^2] + 1.4 y({\rm H_2}) \exp[-12000/(T + 1200)]} \ {\rm cm}^{-3}. \tag{25}$$

Collisional dissociation and ionization absorb the same energy as the binding energy, that is 4.48 eV per H_2 dissociation, 13.6 eV per H ionization, 24.6 eV per He ionization, and 54.4 eV per He^+ ionization.

2.3. Chemical reactions

We solve nonequilibrium chemistry involving the four elements H, He, C and O, that contains the following 45 species: H, H_2, e^-, H^+, H_2^+, H_3^+, H^-, He, He^+, He^{++}, HeH^+, C, C_2, CH, CH_2, CH_3, CH_4, C^+, C_2^+, CH^+, CH_2^+, CH_3^+, CH_4^+, CH_5^+, O, O_2, OH, CO, H_2O, HCO, O_2H, CO_2, H_2CO, H_2O_2, O^+, O_2^+, OH^+, CO^+, H_2O^+, HCO^+, O_2H^+, H_3O^+, H_2CO^+, HCO_2^+ and H_3CO^+. Chemical reactions included are listed in Appendix. The reactions of H and He chemistry are mainly taken from Abel et al. (1997) and Galli & Palla (1998). Other important H_2 forming processes included are the three-body reactions (Palla et al. 1983) and the reaction on the surfaces of the dust grains (Tielens & Hollenbach 1985). In addition, we supplement H, He, C and O chemical reactions involving the above species from Millar, Farquhar, & Willacy (1997).

3. Results

In this section, we present the results obtained by the method described in §2 and discuss our analysis.

Figure 1 displays the evolutionary trajectories of protostellar clouds whose metallicities are $z = 0, 10^{-6}, 10^{-4}, 10^{-2}, 1$. Here we set the initial condition to be $T = 100{\rm K}, n = 1{\rm cm}^{-3}, y(e) =$

$1 \times 10^{-4}, y(H_2) = 1 \times 10^{-6}$. All the carbon is assumed to be in the form of CII, while oxygen is OI at the beginning.

The evolutionary trajectories for two other initial conditions are shown in Figure 2, as well as the same curves in Figure 1. We can see from Figure 2 that trajectories of clouds with a fixed composition converge rapidly toward the dense region for any initial conditions (e.g., Hayashi & Nakano 1965; Low & Lynden-Bell 1976). We have also tested the sensitivity to initial chemical compostions for two cases – (i) where the ionization degree $y(e) = 1 \times 10^{-3}$ and (ii) all the carbon is assumed to be CI,– and have found the results similar to those shown in Figure 2. Hereafter, we discuss only on the case presented in Figure 1.

In general, as seen in Figure 1, the temperatures of lower metallicity clouds are higher because of their lower radiative cooling ability (i.e., lower radiative cooling rate for the same temperature and density) as long as the clouds are transparent to continuum and continue to collapse dynamically, owing to the efficient radiative cooling, in other words, during what is known as the "first collapse" stage.

On account of the total lack of metals and grains, the only cooling agent in the temperature range below $\sim 10^4$K for primordial ($z = 0$) clouds is rovibrational transitions of molecular hydrogen (e.g., Matsuda et al. 1969). In the primordial gas, H_2 is formed mainly by the H^- process,

$$H + e^- \rightarrow H^- + \gamma; \tag{26}$$

$$H + H^- \rightarrow H_2 + e^-, \tag{27}$$

(Saslaw & Zipoy 1967) until the density reaches $\sim 10^8 \mathrm{cm}^{-3}$, where the three-body reactions

$$3H \rightarrow H_2 + H \tag{28}$$

$$2H + H_2 \rightarrow 2H_2 \tag{29}$$

become efficient (Palla et al. 1983). H_2 line emission via electric quadrupole transitions is the only efficient cooling agent until the number density exceeds $\sim 10^{14} \mathrm{cm}^{-3}$, where H_2 continuum emission via collision-induced dipole transitions begins to overwhelm. The drop in temperature at $n \simeq 10^{16} \mathrm{cm}^{-3}$ is due to the quadrature dependence of the collision-induced emission coefficient on the density. The cloud becomes optically thick to the continuum at $10^{16} \mathrm{cm}^{-3}$. (See Fig. 3 a)

The gravitational contraction of metal-free protostellar clouds has been investigated with Omukai & Nishi (1998) by detailed hydrodynamical calculations assuming spherical symmetry. Our evolutionary trajectory for the primordial cloud agrees well with those of Omukai & Nishi (1998) at the number density $n \gtrsim 10^{10} \mathrm{cm}^{-3}$. At lower densities, the temperature of ours is higher owing to the influence of Omukai & Nishi's (1998) initial condition. They started the calculation from a cloud in hydrostatic equilibrium at $n \simeq 10^6 \mathrm{cm}^{-3}$. As long as the density is not so much higher than the initial value, the collapse is slower than the free-fall rate, which we have assumed in this paper. As a result, the temperature is lower because of the lower compressional heating.

The evolution of the cloud with $z = 10^{-6}$ is essentially the same as that of the primordial cloud, although there is minor deviation caused by extra cooling owing to water molecules and dust grains. (See Fig. 3 b) The dust thermal emission dominates the cooling just before the H_2 continuum becomes effective. However, it is only temporary and the grains rapidly sublimate at $n \sim 10^{14} \mathrm{cm}^{-3}$. The most refractory grain composition that contributes to the Planck mean opacity is iron, which sublimate at about 1200K at this density (Table 3 of Pollack et al. 1994). The slight amount of dust grains in the cloud with $z = 10^{-6}$ does not contribute to H_2 formation significantly, as seen in Figure 4.

For the cloud with $z = 10^{-4}$, H_2, which is formed mainly on the grain surfaces instead of the H^- process, is the major coolant at low densities ($< 10^4 \mathrm{cm}^{-3}$). Water molecules, which are mainly formed at $\sim 10^6 \mathrm{cm}^{-3}$ by the reaction

$$H_2 + OH \rightarrow H_2O + H, \tag{30}$$

dominate the cooling in the range $10^5 \mathrm{cm}^{-3} < n < 10^{10} \mathrm{cm}^{-3}$. In present-day molecular cloud cores, usually neither H_2O nor OH plays a key role in the thermal balance since the temperature there is lower than the excitation energy of these molecular species (Neufeld, Lepp, & Melnick 1995). However, in lower metal environments, the temperature is higher because of the lower radiative cooling. In that case, H_2O can be a principal cooling agent. In the cloud with $z = 10^{-4}$, grain surface reactions exceed the H^- process as a mode of H_2 formation, although hydrogen does not become fully molecular until the three-body reaction begins to work. At $10^{10} \mathrm{cm}^{-3}$, the grain thermal emission dominates the cooling and causes the temperature to drop to about 100K. The cloud becomes optically thick to the grain emission at about $10^{13} \mathrm{cm}^{-3}$. (See Fig. 3 c)

For the cloud with $z > 10^{-2}$, cooling is dominated by atomic lines and CO lines in lower densities (that is, $n < 10^6 \mathrm{cm}^{-3}$ for $z = 10^{-2}$, and $n < 10^3 \mathrm{cm}^{-3}$ for $z = 1$, respectively), and by the dust thermal emission in higher densities. (See Fig. 3 d, e) The temperature of our $z = 1$ cloud drops far less than 10K, which is appropriate in present-day protostellar clouds. This is merely because we have ignored external radiation, and the results should not be taken seriously as a model of present-day molecular cloud cores.

Clouds with metallicity $z > 10^{-4}$ become opaque to the thermal radiation of dust grains before the grain vaporization occurs. Once the cloud becomes opaque, it begins to contract adiabatically since the radiative cooling rate drops rapidly. According to some hydrodynamical simulations (e.g, Larson 1969; Masunaga et al. 1998), a transient core in hydrostatic equilibrium (called a "first core") forms after the cloud has more contractions. The hydrostatic core continues the adiabatic contraction by accreting the envelope matter until the temperature reaches ~ 2000 K, where molecular hydrogen begins to dissociate.

Clouds with lower metallicity (i.e., $z < 10^{-6}$) become opaque to the H_2 continuum instead of the dust thermal emission, as described above. Since the temperature at that time is already near the dissociation value, molecular hydrogen begins to dissociate just after the cloud becomes opaque. As a result, no transient hydrostatic core forms in these cases as has been demonstrated by the hydrodynamical calculations of Omukai & Nishi (1998).

When the ratio of specific heats $\Gamma = \mathrm{d}\log p / \mathrm{d}\log\rho$ exceeds the critical value 4/3, corresponding to a gradient of 1/3 in the density-temperature ($n - T$) plane (i.e., Figure 1), the bulk motion of the cloud is decelerated and the free-fall assumption is no longer valid. However, the trajectories in the $n - T$ plane are not altered since the clouds contract almost adiabatically anyway in the opaque stage because of the rapidly declining radiative cooling rate (e.g., Larson 1969; Narita, Nakano, & Hayashi 1970).

In the course of the adiabatic contraction of the transient cores, all the evolutionary trajectories converge to a certain line (Fig. 1, *dashed line*) in spite of their different composition and histories. We discuss the reason for the convergence in the following. The trajectories in the $n - T$ plane just prior to when the clouds become opaque are determined by thermal balance between the compressional heating and the radiative cooling. The compressional heating rate (per unit mass) is given by

$$\mathcal{G}_{\mathrm{comp}} = -p \frac{d}{dt}\left(\frac{1}{\rho}\right) = \frac{c_{\mathrm{s}}^2}{t_{\mathrm{ff}}}, \tag{31}$$

where p is the pressure and c_{s} is the sound speed in the central region of the cloud. The radiative cooling at that time is dominated by continuum for all clouds, namely, the dust thermal emission for clouds with

relative metallicity $z > 10^{-4}$, or the H_2 continuum emission for those with lower metallicity. The radiative cooling rate is given by

$$\mathcal{L}_{\rm rad} = 4\kappa_{\rm B}\sigma T^4, \tag{32}$$

where $\kappa_{\rm B}$ is the Planck mean continuum opacity. In the equation above, we have used the relation that the grain temperature is the same as the gas temperature, $T_{\rm gr} = T$, which is valid in a cloud so dense that it becomes opaque to the continuum. Note that expression (32) holds for any clouds that cool mainly by continuum by choosing an appropriate value of opacity, where the opacity is an increasing function of relative metallicity z. Equating (31) and (32), for each value of $\kappa_{\rm B}(z)$, we obtain a trajectory just before the cloud becomes opaque (we call it ${\rm Tr}(\kappa_{\rm B})$);

$${\rm Tr}(\kappa_{\rm B}): \quad \frac{c_{\rm s}^2}{t_{\rm ff}} = 4\kappa_{\rm B}\sigma T^4. \tag{33}$$

As the cloud of opacity $\kappa_{\rm B}$ collapses along the trajectory represented by (33), the central part of the cloud becomes opaque to the continuum at the point

$${\rm P}(\kappa_{\rm B}): \quad \tau_{\rm J}(\kappa_{\rm B}, n, T) = \kappa_{\rm B}\rho\pi\frac{c_{\rm s}}{\sqrt{G\rho}} = 1, \tag{34}$$

where we have used the assumption that the size of the central region is approximately $\lambda_{\rm J}$. Eliminating $\kappa_{\rm B}$ in equations (33) and (34), we obtain the locus L of points P for variable $\kappa_{\rm B}$;

$${\rm L}: \quad T = \left(\frac{k^3}{12\sigma^2 m_{\rm p}}\right)^{1/5} n^{2/5}. \tag{35}$$

On the other hand, the trajectory of the cloud of opacity $\kappa_{\rm B}$ in the opaque stage, ${\rm O}(\kappa_{\rm B})$, is the line that starts from the point ${\rm P}(\kappa_{\rm B})$ and whose gradient is approximately equal to the value for adiabatic contraction $\gamma_{\rm ad} - 1$. The adiabatic exponent $\gamma_{\rm ad}$ for molecular hydrogen is 7/5 in the temperature range $T \gtrsim 200$K, while it is 2/3 in the lowest temperature. The gradient of the trajectory ${\rm O}(\kappa_{\rm B})$ in the range $T \gtrsim 200$K is 2/5. This value happens to be the same as the gradient of the line L. Thus, the trajectories in the opaque stage O all coincide with the line L, which can be written only by physical constants. When the clouds become opaque (i.e., at the point P), their specific entropy has the same value for all clouds regardless of their metallicity.

As a cloud climbs up along line L, the temperature reaches the dissociation value ($\simeq 2000$K) at $n \simeq 3 \times 10^{16}{\rm cm}^{-3}$. The ratio of specific heats are reduced below the critical value 4/3. Then the cloud begins to collapse dynamically again, or in other words, it begins the second collapse (e.g., Larson 1969). The trajectories in the second collapse stage are also unique because the specific entropy has the same value for all clouds regardless of their metallicity. When most hydrogen molecules have been dissociated, the ratio of specific heats rises above the critical value 4/3 again. After the central part of the cloud contracts almost adiabatically to some extent, a hydrostatic core forms. This core is referred to as the stellar or second core in literature. We cannot accurately estimate the size of the stellar core from our simple one-zone treatment. However, hydrodynamical calculations tell us that the number density and mass of the stellar core at its formation time are on the order of $10^{22}{\rm cm}^{-3}$ and $10^{-3}M_\odot$ respectively, both for present-day (Larson 1969) and primordial protostars (Omukai & Nishi 1998). This value is expected to be universal, namely, independent of metallicity since the equations of state, or trajectories in the $n - T$ plane, are the same in the second collapse stage.

The stellar core, or protostar, grows in mass by accretion of the envelope material. The temperature rises accordingly and eventually the core will become an ordinary star. Consequently, the final mass of stars

is determined by the subsequent accretion onto the core, although the size of the protostar at the time of formation is the same. Stahler, Shu, & Taam (1980) argued that a rough estimate of the protostellar mass accretion rate $\dot{M}$ can be obtained from the relation

$$\dot{M} \sim c_{\rm s}^3/G, \tag{36}$$

where $c_{\rm s}$ is the isothermal sound speed in the initial protostellar cloud. Therefore, the mass accretion rate is higher for a lower metallicity cloud because of the higher temperature of the protostellar cloud (Stahler, Palla, & Salpeter 1986). The higher accretion rate and lower opacity (then smaller radiation force) may result in the higher mass of formed stars for a lower metallicity cloud (e.g., Wolfire & Cassinelli 1987). However, to address these issues fully, further investigations are needed.

4. Summary

We have investigated the thermal and chemical evolution of collapsing protostellar clouds with different metallicities. The varied range of metallicity spans the local interstellar value ($\simeq 1 Z_\odot$) to zero.

The evolution of the clouds is summarized as follows. While the clouds are transparent to continuous radiation, the temperature of clouds with lower metallicity is higher since their radiative cooling rates are lower for the same density and temperature. However, after the clouds become opaque and begin adiabatic contraction, their evolutionary trajectories converge to a line that is determined only by physical constants. Thereafter, the trajectories coincide with each other regardless of their metallicity. Consequently, the physical dimension of the stellar core at the time of formation is the same for clouds with any composition.

We have also discussed analytically the reasons for the convergence.

The author wishes to express his cordial thanks to Humitaka Sato and Naoshi Sugiyama for their continual interest and advice, to Hiroshi Koyama, Ryoichi Nishi, and Toru Tsuribe for useful discussions, and to the referee for improving this manuscript.

Table 1. Chemical Reactions Included

Number	Reaction	Rate Coefficient [a]	Reference [b]
1	$H + e \rightarrow H^+ + 2e$	$k_1 = \exp[-32.71396786 + 13.536556\ln(T(\mathrm{eV}))$ $-5.73932875(\ln(T(\mathrm{eV})))^2$ $+1.56315498(\ln(T(\mathrm{eV})))^3$ $-0.2877056(\ln(T(\mathrm{eV})))^4$ $+3.48255977\times10^{-2}(\ln(T(\mathrm{eV})))^5$ $-2.63197617\times10^{-3}(\ln(T(\mathrm{eV})))^6$ $+1.11954395\times10^{-4}(\ln(T(\mathrm{eV})))^7$ $-2.03914985\times10^{-6}(\ln(T(\mathrm{eV})))^8]$	A97
2	$H^+ + e \rightarrow H + \gamma$	$k_2 = \exp[-28.6130338 - 0.72411256(\ln(T(\mathrm{eV})))$ $-2.02604473\times10^{-2}(\ln(T(\mathrm{eV})))^2$ $-2.38086188\times10^{-3}(\ln(T(\mathrm{eV})))^3$ $-3.21260521\times10^{-4}(\ln(T(\mathrm{eV})))^4$ $-1.42150291\times10^{-5}(\ln(T(\mathrm{eV})))^5$ $+4.98910892\times10^{-6}(\ln(T(\mathrm{eV})))^6$ $+5.75561414\times10^{-7}(\ln(T(\mathrm{eV})))^7$ $-1.85676704\times10^{-8}(\ln(T(\mathrm{eV})))^8$ $-3.07113524\times10^{-9}(\ln(T(\mathrm{eV})))^9]$	A97
3	$He + e \rightarrow He^+ + 2e$	$k_3 = \exp[-44.09864886 + 23.91596563(\ln(T(\mathrm{eV})))$ $-10.7532302(\ln(T(\mathrm{eV})))^2$ $+3.05803875(\ln(T(\mathrm{eV})))^3$ $-0.56851189(\ln(T(\mathrm{eV})))^4$ $+6.79539123\times10^{-2}(\ln(T(\mathrm{eV})))^5$ $-5.00905610\times10^{-3}(\ln(T(\mathrm{eV})))^6$ $+2.06723616\times10^{-4}(\ln(T(\mathrm{eV})))^7$ $-3.64916141\times10^{-6}(\ln(T(\mathrm{eV})))^8]$	A97
4	$He^+ + e \rightarrow He + \gamma$	$k_4 = 3.925\times10^{-13}T(\mathrm{eV})^{-0.6353}$ $+1.544\times10^{-9}T(\mathrm{eV})^{-1.5}$ $[3.0\times10^{-1}\exp(-48.596/T(\mathrm{eV})) + \exp(-40.496/T(\mathrm{eV}))]$	A97
5	$He^+ + e \rightarrow He^{++} + 2e$	$k_5 = \exp[-68.71040990 + 43.93347633(\ln(T(\mathrm{eV})))$ $-18.4806699(\ln(T(\mathrm{eV})))^2$ $+4.70162649(\ln(T(\mathrm{eV})))^3$ $-0.76924663(\ln(T(\mathrm{eV})))^4$ $+8.113042\times10^{-2}(\ln(T(\mathrm{eV})))^5$ $-5.32402063\times10^{-3}(\ln(T(\mathrm{eV})))^6$ $+1.97570531\times10^{-4}(\ln(T(\mathrm{eV})))^7$ $-3.16558106\times10^{-6}(\ln(T(\mathrm{eV})))^8]$	A97
6	$He^{++} + e \rightarrow He^+ + \gamma$	$k_6 = 3.36\times10^{-10}T^{-1/2}(T/10^3)^{-0.2}[1+(T/10^6)^{0.7}]^{-1}$	A97
7	$H + e \rightarrow H^- + \gamma$	$k_7 = 1.4\times10^{-18}T^{0.928}\exp(-T/1.62\times10^4)$	GP98
8	$H^- + H \rightarrow H_2 + e$	$k_8 = 4.0\times10^{-9}T^{-0.17}$ $(T > 300)$ $k_8 = 1.5\times10^{-9}$ $(T < 300)$	GP98
9	$H + H^+ \rightarrow H_2^+ + \gamma$	$k_9 = 10^{[-19.38-1.523\log_{10}T+1.118(\log_{10}T)^2-0.1269(\log_{10}T)^3]}$	GP98

Table 1—Continued

Number	Reaction	Rate Coefficient [a]	Reference [b]
10	$H_2^+ + H \rightarrow H_2 + H^+$	$k_{10} = 6.4 \times 10^{-10}$	GP98
11	$H_2 + H^+ \rightarrow H_2^+ + H$	$k_{11} = 3.0 \times 10^{-10} \exp(-2.1050 \times 10^4/T)$	GP98
12	$H_2 + e \rightarrow 2H + e$	$k_{12} = 4.4 \times 10^{-10} T^{0.35} \exp(-1.02 \times 10^5/T)$	GP98
13	$H_2 + H \rightarrow 3H$	$k_{13} = k_H^{1-a} k_L^a$	
		$k_L = 1.12 \times 10^{-10} \exp(-7.035 \times 10^4/T)$	SK87
		$k_H = 6.5 \times 10^{-7} T^{-1/2}$	
		$\exp(-5.2 \times 10^4/T)[1 - \exp(-6000/T)]$	
		$a = (1 + n/n_{cr})^{-1}$	
		$\log_{10}(n_{cr}) = 4.0 - 0.416 \log_{10}(T/10^4)$	
		$-0.327(\log_{10}(T/10^4))^2$	
14	$H^- + e \rightarrow H + 2e$	$k_{14} = \exp[-18.01849334 + 2.3608522(\ln(T(\mathrm{eV})))$	
		$-0.28274430(\ln(T(\mathrm{eV})))^2$	
		$+1.62331664 \times 10^{-2}(\ln(T(\mathrm{eV})))^3$	
		$-3.36501203 \times 10^{-2}(\ln(T(\mathrm{eV})))^4$	
		$+1.17832978 \times 10^{-2}(\ln(T(\mathrm{eV})))^5$	
		$-1.65619470 \times 10^{-3}(\ln(T(\mathrm{eV})))^6$	
		$+1.06827520 \times 10^{-4}(\ln(T(\mathrm{eV})))^7$	
		$-2.63128581 \times 10^{-6}(\ln(T(\mathrm{eV})))^8]$	A97
15	$H^- + H^+ \rightarrow 2H$	$k_{15} = 5.7 \times 10^{-6} T^{-1/2}$	GP98
		$+ 6.3 \times 10^{-8} - 9.2 \times 10^{-11} T^{1/2} + 4.4 \times 10^{-13} T$	
16	$H^- + H^+ \rightarrow H_2^+ + e$	$k_{16} = 6.9 \times 10^{-9} T^{-0.35} \quad (T < 8000)$	GP98
		$k_{16} = 9.6 \times 10^{-7} T^{-0.9} \quad (T > 8000)$	
17	$H_2^+ + e \rightarrow 2H$	$k_{17} = 2.0 \times 10^{-7} T^{-1/2}$	GP98
18	$H_2^+ + H^- \rightarrow H_2 + H$	$k_{18} = 2.30 \times 10^{-7} (T/300)^{-1/2}$	M97
19	$3H \rightarrow H_2 + H$	$k_{19} = 5.5 \times 10^{-29} T^{-1}$	PSS83
20	$2H + H_2 \rightarrow 2H_2$	$k_{20} = k_{19}/8$	PSS83
21	$2H_2 \rightarrow 2H + H_2$	$k_{21} = k_H^{1-a} k_L^a$	SK87
		$k_L = 1.18 \times 10^{-10} \exp(-6.95 \times 10^4/T)$	PSS83 (k_H)
		$k_H = 8.125 \times 10^{-8} T^{-1/2}$	
		$\exp(-5.2 \times 10^4/T)[1 - \exp(-6.0 \times 10^3/T)]$	
		$a = (1 + n/n_{cr})^{-1}$	
		$\log_{10}(n_{cr}) = 4.845 - 1.3 \log_{10}(T/10^4)$	
		$+1.62(\log_{10}(T/10^4))^2$	
22	$2H \rightarrow H^+ + e + H$	$k_{22} = 1.7 \times 10^{-4} k_1$	PSS83
23	$2H + \mathrm{grain} \rightarrow H_2$	$k_{23} = 6.0 \times 10^{-17} (T/300\mathrm{K})^{1/2} f_a$	TH85
		$\times[1 + 4.0 \times 10^{-2}(T + T_{gr})^{1/2}$	
		$+2.0 \times 10^{-3} T + 8.0 \times 10^{-6} T^2]^{-1}$	
		$\times Z/Z_{local}$	
		$f_a = [1 + \exp(7.5 \times 10^2 (1/75 - 1/T_{gr}))]^{-1}$	
24	$He^+ + H_2 \rightarrow H^+ + H + He$	$k_{24} = 3.70 \times 10^{-14} \exp(-35/\mathrm{T})$	M97
25	$H_2^+ + He \rightarrow HeH^+ + H$	$k_{25} = 1.30 \times 10^{-10}$	M97

Table 1—Continued

Number	Reaction	Rate Coefficient [a]	Reference [b]
26	$H_2^+ + H_2 \rightarrow H_3^+ + H$	$k_{26} = 2.08 \times 10^{-9}$	M97
27	$H_3^+ + H^- \rightarrow 2H_2$	$k_{27} = 2.30 \times 10^{-7}(T/300)^{-0.50}$	M97
28	$He^+ + H \rightarrow H^+ + He$	$k_{28} = 1.90 \times 10^{-15}$	M97
29	$He^+ + H^- \rightarrow H + He$	$k_{29} = 2.30 \times 10^{-7}(T/300)^{-0.50}$	M97
30	$He^+ + H_2 \rightarrow H_2^+ + He$	$k_{30} = 7.20 \times 10^{-15}$	M97
31	$HeH^+ + H \rightarrow H_2^+ + He$	$k_{31} = 9.10 \times 10^{-10}$	M97
32	$HeH^+ + H_2 \rightarrow H_3^+ + He$	$k_{32} = 1.50 \times 10^{-9}$	M97
33	$H_3^+ + e \rightarrow H_2 + H$	$k_{33} = 1.50 \times 10^{-8}(T/300)^{-0.50}$	M97
34	$H_3^+ + e \rightarrow 3H$	$k_{34} = 1.50 \times 10^{-8}(T/300)^{-0.50}$	M97
35	$HeH^+ + e \rightarrow H + He$	$k_{35} = 2.00 \times 10^{-7}(T/300)^{-0.50}$	M97
36	$H + CH \rightarrow C + H_2$	$k_{36} = 4.98 \times 10^{-11}$	M97
37	$H + CH \rightarrow C + 2H$	$k_{37} = 6.00 \times 10^{-9}\exp(-40200/T)$	M97
38	$H + CH_2 \rightarrow CH + H_2$	$k_{38} = 2.70 \times 10^{-10}$	M97
39	$H + CH_3 \rightarrow CH_2 + H_2$	$k_{39} = 1.00 \times 10^{-10}\exp(-7600/T)$	M97
40	$H + CH_4 \rightarrow H_2 + CH_3$	$k_{40} = 5.82 \times 10^{-13}(T/300)^{3.00}\exp(-4045/T)$	M97
41	$H + OH \rightarrow H_2 + O$	$k_{41} = 7.00 \times 10^{-14}(T/300)^{2.80}\exp(-1950/T)$	M97
42	$H + OH \rightarrow O + 2H$	$k_{42} = 6.00 \times 10^{-9}\exp(-50900/T)$	M97
43	$H + H_2O \rightarrow OH + H_2$	$k_{43} = 6.83 \times 10^{-12}(T/300)^{1.60}\exp(-9720/T)$	M97
44	$H + H_2O \rightarrow OH + 2H$	$k_{44} = 5.80 \times 10^{-9}\exp(-52900/T)$	M97
45	$H + C_2 \rightarrow CH + C$	$k_{45} = 4.67 \times 10^{-10}(T/300)^{0.50}\exp(-30450/T)$	M97
46	$H + CO \rightarrow C + OH$	$k_{46} = 1.10 \times 10^{-10}(T/300)^{0.50}\exp(-77700/T)$	M97
47	$H + H_2CO \rightarrow HCO + H_2$	$k_{47} = 1.50 \times 10^{-11}(T/300)^{1.05}\exp(-1650/T)$	M97
48	$H + O_2 \rightarrow OH + O$	$k_{48} = 3.30 \times 10^{-10}\exp(-8460/T)$	M97
49	$H + O_2 \rightarrow 2O + H$	$k_{49} = 6.00 \times 10^{-9}\exp(-52300/T)$	M97
50	$H + O_2H \rightarrow H_2O + O$	$k_{50} = 5.00 \times 10^{-11}\exp(-866/T)$	M97
51	$H + O_2H \rightarrow H_2 + O2$	$k_{51} = 7.10 \times 10^{-11}\exp(-710/T)$	M97
52	$H + O_2H \rightarrow 2OH$	$k_{52} = 2.80 \times 10^{-10}\exp(-440/T)$	M97
53	$H + H_2O_2 \rightarrow O_2H + H_2$	$k_{53} = 2.80 \times 10^{-12}\exp(-1890/T)$	M97
54	$H + CO_2 \rightarrow OH + CO$	$k_{54} = 2.50 \times 10^{-10}\exp(-13300/T)$	M97
55	$C + H_2 \rightarrow CH + H$	$k_{55} = 6.64 \times 10^{-10}\exp(-11700/T)$	M97
56	$C + OH \rightarrow CH + O$	$k_{56} = 2.25 \times 10^{-11}(T/300)^{0.50}\exp(-14800/T)$	M97
57	$C + CO \rightarrow C_2 + O$	$k_{57} = 2.94 \times 10^{-11}(T/300)^{0.50}\exp(-58025/T)$	M97
58	$O + H_2 \rightarrow OH + H$	$k_{58} = 3.43 \times 10^{-13}(T/300)^{2.67}\exp(-3160/T)$	M97
59	$O + CH \rightarrow OH + C$	$k_{59} = 2.52 \times 10^{-11}\exp(-2381/T)$	M97
60	$O + CH_2 \rightarrow CH + OH$	$k_{60} = 4.98 \times 10^{-10}\exp(-6000/T)$	M97
61	$O + CH_2 \rightarrow HCO + H$	$k_{61} = 1.44 \times 10^{-11}(T/300)^{0.50}\exp(-2000/T)$	M97
62	$O + CH_4 \rightarrow CH_3 + OH$	$k_{62} = 8.32 \times 10^{-12}(T/300)^{1.56}\exp(-4270/T)$	M97
63	$O + H_2O \rightarrow 2OH$	$k_{63} = 1.85 \times 10^{-11}(T/300)^{0.95}\exp(-8571/T)$	M97
64	$O + H_2CO \rightarrow HCO + OH$	$k_{64} = 1.78 \times 10^{-11}(T/300)^{0.57}\exp(-1390/T)$	M97
65	$O + H_2O_2 \rightarrow O_2H + OH$	$k_{65} = 1.40 \times 10^{-12}\exp(-2000/T)$	M97
66	$O + CO_2 \rightarrow CO + O_2$	$k_{66} = 2.80 \times 10^{-11}\exp(-26500/T)$	M97

Table 1—Continued

Number	Reaction	Rate Coefficient [a]	Reference [b]
67	$H^+ + O \rightarrow O^+ + H$	$k_{67} = 7.00 \times 10^{-10}\exp(-232/T)$	M97
68	$H_2 + C \rightarrow CH_2 + \gamma$	$k_{68} = 1.00 \times 10^{-17}$	M97
69	$H_2 + CH \rightarrow CH_2 + H$	$k_{69} = 2.38 \times 10^{-10}\exp(-1760/T)$	M97
70	$H_2 + CH \rightarrow C + H + H_2$	$k_{70} = 6.00 \times 10^{-9}\exp(-40200/T)$	M97
71	$H_2 + CH_2 \rightarrow CH_3 + H$	$k_{71} = 5.18 \times 10^{-11}(T/300)^{0.17}\exp(-6400/T)$	M97
72	$H_2 + CH_3 \rightarrow CH_4 + H$	$k_{72} = 6.86 \times 10^{-14}(T/300)^{2.74}\exp(-4740/T)$	M97
73	$H_2 + OH \rightarrow H_2O + H$	$k_{73} = 1.55 \times 10^{-12}(T/300)^{1.60}\exp(-1660/T)$	M97
74	$H_2 + OH \rightarrow O + H + H_2$	$k_{74} = 6.00 \times 10^{-9}\exp(-50900/T)$	M97
75	$H_2 + H_2O \rightarrow OH + H + H_2$	$k_{75} = 5.80 \times 10^{-9}\exp(-52900/T)$	M97
76	$H_2 + O_2 \rightarrow O_2H + H$	$k_{76} = 2.40 \times 10^{-10}\exp(-28500/T)$	M97
77	$H_2 + O_2 \rightarrow 2OH$	$k_{77} = 3.16 \times 10^{-10}\exp(-21890/T)$	M97
78	$H_2 + O_2 \rightarrow 2O + H_2$	$k_{78} = 6.00 \times 10^{-9}\exp(-52300/T)$	M97
79	$H_2 + O_2H \rightarrow H_2O_2 + H$	$k_{79} = 1.20 \times 10^{-12}\exp(-9400/T)$	M97
80	$H_2 + CO_2 \rightarrow H_2O + CO$	$k_{80} = 2.94 \times 10^{-14}(T/300)^{0.50}\exp(-7550/T)$	M97
81	$H_3^+ + O_2 \rightarrow O_2H^+ + H_2$	$k_{81} = 5.00 \times 10^{-9}\exp(-150/T)$	M97
82	$C^+ + H_2 \rightarrow CH^+ + H$	$k_{82} = 1.00 \times 10^{-10}\exp(-4640/T)$	M97
83	$CH + CH_4 \rightarrow CH_2 + CH_3$	$k_{83} = 2.28 \times 10^{-11}(T/300)^{0.70}\exp(-3000/T)$	M97
84	$CH + OH \rightarrow HCO + H$	$k_{84} = 1.44 \times 10^{-11}(T/300)^{0.50}\exp(-5000/T)$	M97
85	$CH + HCO \rightarrow CH_2 + CO$	$k_{85} = 2.87 \times 10^{-12}(T/300)^{0.70}\exp(-500/T)$	M97
86	$CH + H_2CO \rightarrow CH_2 + HCO$	$k_{86} = 9.21 \times 10^{-12}(T/300)^{0.70}\exp(-2000/T)$	M97
87	$CH + O_2 \rightarrow HCO + O$	$k_{87} = 1.44 \times 10^{-11}(T/300)^{0.50}\exp(-3000/T)$	M97
88	$CH + O_2H \rightarrow CH_2 + O_2$	$k_{88} = 2.94 \times 10^{-13}(T/300)^{0.50}\exp(-7550/T)$	M97
89	$CH + O_2H \rightarrow HCO + OH$	$k_{89} = 1.44 \times 10^{-11}(T/300)^{0.50}\exp(-3000/T)$	M97
90	$CH + CO_2 \rightarrow HCO + CO$	$k_{90} = 2.94 \times 10^{-13}(T/300)^{0.50}\exp(-3000/T)$	M97
91	$2CH_2 \rightarrow CH + CH_3$	$k_{91} = 4.00 \times 10^{-10}\exp(-5000/T)$	M97
92	$CH_2 + CH_4 \rightarrow 2CH_3$	$k_{92} = 7.13 \times 10^{-12}\exp(-5050/T)$	M97
93	$CH_2 + HCO \rightarrow CH_3 + CO$	$k_{93} = 3.00 \times 10^{-11}$	M97
94	$CH_2 + H_2CO \rightarrow CH_3 + HCO$	$k_{94} = 3.30 \times 10^{-13}\exp(-3270/T)$	M97
95	$CH_2^+ + H \rightarrow CH^+ + H_2$	$k_{95} = 1.00 \times 10^{-9}\exp(-7080/T)$	M97
96	$CH_3 + H_2CO \rightarrow CH_4 + HCO$	$k_{96} = 2.94 \times 10^{-13}(T/300)^{0.50}\exp(-3000/T)$	M97
97	$CH_3^+ + H \rightarrow CH_2^+ + H_2$	$k_{97} = 7.00 \times 10^{-10}\exp(-10560/T)$	M97
98	$OH + CH_2 \rightarrow CH_3 + O$	$k_{98} = 1.44 \times 10^{-11}(T/300)^{0.50}\exp(-3000/T)$	M97
99	$OH + CH_2 \rightarrow H_2O + CH$	$k_{99} = 1.44 \times 10^{-11}(T/300)^{0.50}\exp(-3000/T)$	M97
100	$OH + CH_2 \rightarrow H_2CO + H$	$k_{100} = 3.00 \times 10^{-11}$	M97
101	$OH + CH_3 \rightarrow H_2O + CH_2$	$k_{101} = 5.42 \times 10^{-11}(T/300)^{0.70}\exp(-1000/T)$	M97
102	$OH + CH_4 \rightarrow H_2O + CH_3$	$k_{102} = 8.87 \times 10^{-13}(T/300)^{1.83}\exp(-1400/T)$	M97
103	$2OH \rightarrow H_2O + O$	$k_{103} = 1.65 \times 10^{-12}(T/300)^{1.14}\exp(-50/T)$	M97
104	$OH + CO \rightarrow CO_2 + H$	$k_{104} = 1.00 \times 10^{-13}$	M97
105	$OH + H_2O_2 \rightarrow H_2O + O_2H$	$k_{105} = 1.30 \times 10^{-11}\exp(-670/T)$	M97
106	$H_2O + CH_3 \rightarrow CH_4 + OH$	$k_{106} = 1.20 \times 10^{-14}(T/300)^{2.90}\exp(-7480/T)$	M97
107	$CO + O_2 \rightarrow CO_2 + O$	$k_{107} = 4.20 \times 10^{-12}\exp(-24000/T)$	M97

Table 1—Continued

Number	Reaction	Rate Coefficient [a]	Reference [b]
108	$CO + O_2H \rightarrow CO_2 + OH$	$k_{108} = 2.50 \times 10^{-10}\exp(-11900/T)$	M97
109	$O_2 + CH_2 \rightarrow HCO + OH$	$k_{109} = 4.10 \times 10^{-11}\exp(-750/T)$	M97
110	$O_2 + CH_2 \rightarrow H_2CO + O$	$k_{110} = 1.44 \times 10^{-11}(T/300)^{0.50}\exp(-3500/T)$	M97
111	$O_2 + CH_3 \rightarrow O_2H + CH_2$	$k_{111} = 5.30 \times 10^{-12}\exp(-34975/T)$	M97
112	$O_2 + CH_3 \rightarrow H_2CO + OH$	$k_{112} = 5.50 \times 10^{-13}\exp(-4500/T)$	M97
113	$O_2 + CH_4 \rightarrow CH_3 + O_2H$	$k_{113} = 6.60 \times 10^{-11}\exp(-28630/T)$	M97
114	$O_2 + HCO \rightarrow O_2H + CO$	$k_{114} = 8.50 \times 10^{-11}\exp(-850/T)$	M97
115	$O_2H + CH_3 \rightarrow CH_4 + O_2$	$k_{115} = 6.00 \times 10^{-12}$	M97
116	$O_2H + H_2O \rightarrow H_2O_2 + OH$	$k_{116} = 4.60 \times 10^{-11}\exp(-16500/T)$	M97
117	$O_2H + HCO \rightarrow H_2CO + O_2$	$k_{117} = 5.00 \times 10^{-11}$	M97
118	$O_2H + H_2CO \rightarrow H_2O_2 + HCO$	$k_{118} = 3.30 \times 10^{-12}\exp(-5870/T)$	M97
119	$2O_2H \rightarrow H_2O_2 + O_2$	$k_{119} = 3.10 \times 10^{-12}\exp(-775/T)$	M97
120	$H + HCO \rightarrow CO + H_2$	$k_{120} = 1.50 \times 10^{-10}$	M97
121	$C + H \rightarrow CH + \gamma$	$k_{121} = 1.00 \times 10^{-17}$	M97
122	$2C \rightarrow C_2 + \gamma$	$k_{122} = 1.00 \times 10^{-17}$	M97
123	$C + O \rightarrow CO + \gamma$	$k_{123} = 2.10 \times 10^{-19}$	M97
124	$C + CH \rightarrow C_2 + H$	$k_{124} = 1.73 \times 10^{-11}$	M97
125	$C + OH \rightarrow CO + H$	$k_{125} = 1.10 \times 10^{-10}(T/300)^{0.50}$	M97
126	$C + HCO \rightarrow CH + CO$	$k_{126} = 1.00 \times 10^{-11}$	M97
127	$C + O_2 \rightarrow CO + O$	$k_{127} = 3.30 \times 10^{-11}$	M97
128	$CH_3 + HCO \rightarrow CH_4 + CO$	$k_{128} = 2.00 \times 10^{-10}$	M97
129	$O + H \rightarrow OH + \gamma$	$k_{129} = 9.90 \times 10^{-19}(T/300)^{-0.38}$	M97
130	$2O \rightarrow O_2 + \gamma$	$k_{130} = 4.90 \times 10^{-20}(T/300)^{1.58}$	M97
131	$O + CH \rightarrow CO + H$	$k_{131} = 6.60 \times 10^{-11}$	M97
132	$O + CH \rightarrow HCO^+ + e$	$k_{132} = 2.00 \times 10^{-11}(T/300)^{0.44}$	M97
133	$O + CH_2 \rightarrow CO + 2H$	$k_{133} = 2.00 \times 10^{-10}$	M97
134	$O + CH_3 \rightarrow H_2CO + H$	$k_{134} = 1.40 \times 10^{-10}$	M97
135	$O + OH \rightarrow O_2 + H$	$k_{135} = 4.34 \times 10^{-11}(T/300)^{-0.50}\exp(-30/T)$	M97
136	$O + C_2 \rightarrow CO + C$	$k_{136} = 5.00 \times 10^{-11}(T/300)^{0.50}$	M97
137	$O + HCO \rightarrow CO_2 + H$	$k_{137} = 5.00 \times 10^{-11}$	M97
138	$O + HCO \rightarrow OH + CO$	$k_{138} = 5.00 \times 10^{-11}$	M97
139	$O + O_2H \rightarrow OH + O_2$	$k_{139} = 5.40 \times 10^{-11}$	M97
140	$OH + HCO \rightarrow H_2O + CO$	$k_{140} = 1.70 \times 10^{-10}$	M97
141	$OH + H_2CO \rightarrow H_2O + HCO$	$k_{141} = 4.98 \times 10^{-11}(T/300)\exp(-601/T)$	M97
142	$OH + O_2H \rightarrow H_2O + O_2$	$k_{142} = 4.00 \times 10^{-11}$	M97
143	$2HCO \rightarrow H_2CO + CO$	$k_{143} = 5.00 \times 10^{-11}$	M97
144	$H^+ + CH \rightarrow CH^+ + H$	$k_{144} = 1.90 \times 10^{-9}$	M97
145	$H^+ + CH_2 \rightarrow CH^+ + H_2$	$k_{145} = 1.40 \times 10^{-9}$	M97
146	$H^+ + CH_2 \rightarrow CH_2^+ + H$	$k_{146} = 1.40 \times 10^{-9}$	M97
147	$H^+ + CH_3 \rightarrow CH_3^+ + H$	$k_{147} = 3.40 \times 10^{-9}$	M97
148	$H^+ + CH_4 \rightarrow CH_3^+ + H_2$	$k_{148} = 2.30 \times 10^{-9}$	M97

Table 1—Continued

Number	Reaction	Rate Coefficient [a]	Reference [b]
149	$H^+ + CH_4 \rightarrow CH_4^+ + H$	$k_{149} = 1.50 \times 10^{-9}$	M97
150	$H^+ + OH \rightarrow OH^+ + H$	$k_{150} = 2.10 \times 10^{-9}$	M97
151	$H^+ + H_2O \rightarrow H_2O^+ + H$	$k_{151} = 6.90 \times 10^{-9}$	M97
152	$H^+ + C_2 \rightarrow C_2^+ + H$	$k_{152} = 3.10 \times 10^{-9}$	M97
153	$H^+ + HCO \rightarrow CO^+ + H_2$	$k_{153} = 9.40 \times 10^{-10}$	M97
154	$H^+ + HCO \rightarrow H_2^+ + CO$	$k_{154} = 9.40 \times 10^{-10}$	M97
155	$H^+ + HCO \rightarrow HCO^+ + H$	$k_{155} = 9.40 \times 10^{-10}$	M97
156	$H^+ + H_2CO \rightarrow H_2CO^+ + H$	$k_{156} = 2.96 \times 10^{-9}$	M97
157	$H^+ + H_2CO \rightarrow HCO^+ + H_2$	$k_{157} = 3.57 \times 10^{-9}$	M97
158	$H^+ + O_2 \rightarrow O_2^+ + H$	$k_{158} = 2.00 \times 10^{-9}$	M97
159	$H^+ + CO_2 \rightarrow HCO^+ + O$	$k_{159} = 3.50 \times 10^{-9}$	M97
160	$H^- + C \rightarrow CH + e$	$k_{160} = 1.00 \times 10^{-9}$	M97
161	$H^- + O \rightarrow OH + e$	$k_{161} = 1.00 \times 10^{-9}$	M97
162	$H^- + CH \rightarrow CH_2 + e$	$k_{162} = 1.00 \times 10^{-10}$	M97
163	$H^- + CH_2 \rightarrow CH_3 + e$	$k_{163} = 1.00 \times 10^{-9}$	M97
164	$H^- + CH_3 \rightarrow CH_4 + e$	$k_{164} = 1.00 \times 10^{-9}$	M97
165	$H^- + OH \rightarrow H_2O + e$	$k_{165} = 1.00 \times 10^{-10}$	M97
166	$H^- + CO \rightarrow HCO + e$	$k_{166} = 5.00 \times 10^{-11}$	M97
167	$H^- + HCO \rightarrow H_2CO + e$	$k_{167} = 1.00 \times 10^{-9}$	M97
168	$H_2^+ + C \rightarrow CH^+ + H$	$k_{168} = 2.40 \times 10^{-9}$	M97
169	$H_2^+ + O \rightarrow OH^+ + H$	$k_{169} = 1.50 \times 10^{-9}$	M97
170	$H_2^+ + CH \rightarrow CH^+ + H_2$	$k_{170} = 7.10 \times 10^{-10}$	M97
171	$H_2^+ + CH \rightarrow CH_2^+ + H$	$k_{171} = 7.10 \times 10^{-10}$	M97
172	$H_2^+ + CH_2 \rightarrow CH_3^+ + H$	$k_{172} = 1.00 \times 10^{-9}$	M97
173	$H_2^+ + CH_2 \rightarrow CH_2^+ + H_2$	$k_{173} = 1.00 \times 10^{-9}$	M97
174	$H_2^+ + CH_4 \rightarrow CH_4^+ + H_2$	$k_{174} = 1.40 \times 10^{-9}$	M97
175	$H_2^+ + CH_4 \rightarrow CH5^+ + H$	$k_{175} = 1.14 \times 10^{-10}$	M97
176	$H_2^+ + CH_4 \rightarrow CH_3^+ + H + H_2$	$k_{176} = 2.30 \times 10^{-9}$	M97
177	$H_2^+ + OH \rightarrow OH^+ + H_2$	$k_{177} = 7.60 \times 10^{-10}$	M97
178	$H_2^+ + OH \rightarrow H_2O^+ + H$	$k_{178} = 7.60 \times 10^{-10}$	M97
179	$H_2^+ + H_2O \rightarrow H_2O^+ + H_2$	$k_{179} = 3.90 \times 10^{-9}$	M97
180	$H_2^+ + H_2O \rightarrow H_3O^+ + H$	$k_{180} = 3.40 \times 10^{-9}$	M97
181	$H_2^+ + C_2 \rightarrow C_2^+ + H_2$	$k_{181} = 1.10 \times 10^{-9}$	M97
182	$H_2^+ + CO \rightarrow CO^+ + H_2$	$k_{182} = 6.40 \times 10^{-10}$	M97
183	$H_2^+ + CO \rightarrow HCO^+ + H$	$k_{183} = 2.16 \times 10^{-9}$	M97
184	$H_2^+ + HCO \rightarrow H_3^+ + CO$	$k_{184} = 1.00 \times 10^{-9}$	M97
185	$H_2^+ + HCO \rightarrow HCO^+ + H_2$	$k_{185} = 1.00 \times 10^{-9}$	M97
186	$H_2^+ + H_2CO \rightarrow H_2CO^+ + H_2$	$k_{186} = 1.40 \times 10^{-9}$	M97
187	$H_2^+ + H_2CO \rightarrow HCO^+ + H + H_2$	$k_{187} = 1.40 \times 10^{-9}$	M97
188	$H_2^+ + O_2 \rightarrow O_2H^+ + H$	$k_{188} = 1.90 \times 10^{-9}$	M97
189	$H_2^+ + O_2 \rightarrow O_2^+ + H_2$	$k_{189} = 8.00 \times 10^{-10}$	M97

Table 1—Continued

Number	Reaction	Rate Coefficient [a]	Reference [b]
190	$H_2^+ + CO_2 \rightarrow HCO_2^+ + H$	$k_{190} = 2.35 \times 10^{-9}$	M97
191	$H_3^+ + C \rightarrow CH^+ + H_2$	$k_{191} = 2.00 \times 10^{-9}$	M97
192	$H_3^+ + O \rightarrow OH^+ + H_2$	$k_{192} = 8.00 \times 10^{-10}$	M97
193	$H_3^+ + CH \rightarrow CH_2^+ + H_2$	$k_{193} = 1.20 \times 10^{-9}$	M97
194	$H_3^+ + CH_2 \rightarrow CH_3^+ + H_2$	$k_{194} = 1.70 \times 10^{-9}$	M97
195	$H_3^+ + CH_3 \rightarrow CH_4^+ + H_2$	$k_{195} = 2.10 \times 10^{-9}$	M97
196	$H_3^+ + CH_4 \rightarrow CH5^+ + H_2$	$k_{196} = 2.40 \times 10^{-9}$	M97
197	$H_3^+ + OH \rightarrow H_2O^+ + H_2$	$k_{197} = 1.30 \times 10^{-9}$	M97
198	$H_3^+ + H_2O \rightarrow H_3O^+ + H_2$	$k_{198} = 5.90 \times 10^{-9}$	M97
199	$H_3^+ + CO \rightarrow HCO^+ + H_2$	$k_{199} = 1.73 \times 10^{-9}$	M97
200	$H_3^+ + HCO \rightarrow H_2CO^+ + H_2$	$k_{200} = 1.70 \times 10^{-9}$	M97
201	$H_3^+ + H_2CO \rightarrow H_3CO^+ + H_2$	$k_{201} = 6.30 \times 10^{-9}$	M97
202	$H_3^+ + CO_2 \rightarrow HCO_2^+ + H_2$	$k_{202} = 2.00 \times 10^{-9}$	M97
203	$He^+ + CH \rightarrow C^+ + H + He$	$k_{203} = 1.10 \times 10^{-9}$	M97
204	$He^+ + CH \rightarrow CH^+ + He$	$k_{204} = 5.00 \times 10^{-10}$	M97
205	$He^+ + CH_2 \rightarrow CH^+ + H + He$	$k_{205} = 7.50 \times 10^{-10}$	M97
206	$He^+ + CH_2 \rightarrow C^+ + H_2 + He$	$k_{206} = 7.50 \times 10^{-10}$	M97
207	$He^+ + CH_3 \rightarrow CH^+ + H_2 + He$	$k_{207} = 1.80 \times 10^{-9}$	M97
208	$He^+ + CH_4 \rightarrow CH_3 + H^+ + He$	$k_{208} = 4.80 \times 10^{-10}$	M97
209	$He^+ + CH_4 \rightarrow CH^+ + H_2 + He + H$	$k_{209} = 2.40 \times 10^{-10}$	M97
210	$He^+ + CH_4 \rightarrow CH_2^+ + H_2 + He$	$k_{210} = 9.50 \times 10^{-10}$	M97
211	$He^+ + CH_4 \rightarrow CH_3^+ + He + H$	$k_{211} = 8.50 \times 10^{-11}$	M97
212	$He^+ + CH_4 \rightarrow CH_4^+ + He$	$k_{212} = 5.10 \times 10^{-11}$	M97
213	$He^+ + OH \rightarrow O^+ + H + He$	$k_{213} = 1.10 \times 10^{-9}$	M97
214	$He^+ + H_2O \rightarrow H^+ + OH + He$	$k_{214} = 2.04 \times 10^{-10}$	M97
215	$He^+ + H_2O \rightarrow OH^+ + H + He$	$k_{215} = 2.86 \times 10^{-10}$	M97
216	$He^+ + H_2O \rightarrow H_2O^+ + He$	$k_{216} = 6.05 \times 10^{-11}$	M97
217	$He^+ + C_2 \rightarrow C^+ + C + He$	$k_{217} = 1.60 \times 10^{-9}$	M97
218	$He^+ + C_2 \rightarrow C_2^+ + He$	$k_{218} = 5.00 \times 10^{-10}$	M97
219	$He^+ + CO \rightarrow C^+ + O + He$	$k_{219} = 1.60 \times 10^{-9}$	M97
220	$He^+ + HCO \rightarrow CO^+ + H + He$	$k_{220} = 4.90 \times 10^{-10}$	M97
221	$He^+ + HCO \rightarrow CH^+ + O + He$	$k_{221} = 4.90 \times 10^{-10}$	M97
222	$He^+ + HCO \rightarrow HeH^+ + CO$	$k_{222} = 3.00 \times 10^{-10}$	M97
223	$He^+ + H_2CO \rightarrow CO^+ + H_2 + He$	$k_{223} = 1.88 \times 10^{-9}$	M97
224	$He^+ + H_2CO \rightarrow HCO^+ + H + He$	$k_{224} = 1.14 \times 10^{-9}$	M97
225	$He^+ + O_2 \rightarrow O^+ + O + He$	$k_{225} = 1.00 \times 10^{-9}$	M97
226	$He^+ + O_2 \rightarrow O_2^+ + He$	$k_{226} = 3.30 \times 10^{-11}$	M97
227	$He^+ + CO_2 \rightarrow O_2^+ + C + He$	$k_{227} = 1.10 \times 10^{-11}$	M97
228	$He^+ + CO_2 \rightarrow O^+ + CO + He$	$k_{228} = 1.00 \times 10^{-10}$	M97
229	$He^+ + CO_2 \rightarrow CO^+ + O + He$	$k_{229} = 8.70 \times 10^{-10}$	M97
230	$He^+ + CO_2 \rightarrow C^+ + O_2 + He$	$k_{230} = 4.00 \times 10^{-11}$	M97

Table 1—Continued

Number	Reaction	Rate Coefficient [a]	Reference [b]
231	$C^+ + H \rightarrow CH^+ + \gamma$	$k_{231} = 1.70 \times 10^{-17}$	M97
232	$C^+ + O \rightarrow CO^+ + \gamma$	$k_{232} = 2.50 \times 10^{-18}$	M97
233	$C^+ + H^- \rightarrow H + C$	$k_{233} = 2.30 \times 10^{-7}(T/300)^{-0.50}$	M97
234	$C^+ + H_2 \rightarrow CH_2^+ + \gamma$	$k_{234} = 4.00 \times 10^{-16}(T/300)^{-0.20}$	M97
235	$C^+ + CH \rightarrow C_2^+ + H$	$k_{235} = 3.80 \times 10^{-10}$	M97
236	$C^+ + CH \rightarrow CH^+ + C$	$k_{236} = 3.80 \times 10^{-10}$	M97
237	$C^+ + CH_2 \rightarrow CH_2^+ + C$	$k_{237} = 5.20 \times 10^{-10}$	M97
238	$C^+ + OH \rightarrow CO^+ + H$	$k_{238} = 7.70 \times 10^{-10}$	M97
239	$C^+ + H_2O \rightarrow HCO^+ + H$	$k_{239} = 2.70 \times 10^{-9}$	M97
240	$C^+ + HCO \rightarrow HCO^+ + C$	$k_{240} = 4.80 \times 10^{-10}$	M97
241	$C^+ + HCO \rightarrow CH^+ + CO$	$k_{241} = 4.80 \times 10^{-10}$	M97
242	$C^+ + H_2CO \rightarrow CH_2^+ + CO$	$k_{242} = 2.34 \times 10^{-9}$	M97
243	$C^+ + H_2CO \rightarrow HCO^+ + CH$	$k_{243} = 7.80 \times 10^{-10}$	M97
244	$C^+ + H_2CO \rightarrow H_2CO^+ + C$	$k_{244} = 7.80 \times 10^{-10}$	M97
245	$C^+ + O_2 \rightarrow CO^+ + O$	$k_{245} = 3.80 \times 10^{-10}$	M97
246	$C^+ + O_2 \rightarrow O^+ + CO$	$k_{246} = 6.20 \times 10^{-10}$	M97
247	$C^+ + CO_2 \rightarrow CO^+ + CO$	$k_{247} = 1.10 \times 10^{-9}$	M97
248	$CH^+ + H \rightarrow C^+ + H_2$	$k_{248} = 7.50 \times 10^{-10}(T/300)^{-0.50}$	M97
249	$CH^+ + C \rightarrow C_2^+ + H$	$k_{249} = 1.20 \times 10^{-9}$	M97
250	$CH^+ + O \rightarrow CO^+ + H$	$k_{250} = 3.50 \times 10^{-10}$	M97
251	$CH^+ + H_2 \rightarrow CH_2^+ + H$	$k_{251} = 1.20 \times 10^{-9}$	M97
252	$CH^+ + CH \rightarrow C_2^+ + H_2$	$k_{252} = 7.40 \times 10^{-10}$	M97
253	$CH^+ + OH \rightarrow CO^+ + H_2$	$k_{253} = 7.50 \times 10^{-10}$	M97
254	$CH^+ + H_2O \rightarrow HCO^+ + H_2$	$k_{254} = 2.90 \times 10^{-9}$	M97
255	$CH^+ + H_2O \rightarrow H_3O^+ + C$	$k_{255} = 5.80 \times 10^{-10}$	M97
256	$CH^+ + H_2O \rightarrow H_2CO^+ + H$	$k_{256} = 5.80 \times 10^{-10}$	M97
257	$CH^+ + CO \rightarrow HCO^+ + C$	$k_{257} = 7.00 \times 10^{-12}$	M97
258	$CH^+ + HCO \rightarrow CH_2^+ + CO$	$k_{258} = 4.60 \times 10^{-10}$	M97
259	$CH^+ + HCO \rightarrow HCO^+ + CH$	$k_{259} = 4.60 \times 10^{-10}$	M97
260	$CH^+ + H_2CO \rightarrow CH_3^+ + CO$	$k_{260} = 9.60 \times 10^{-10}$	M97
261	$CH^+ + H_2CO \rightarrow HCO^+ + CH_2$	$k_{261} = 9.60 \times 10^{-10}$	M97
262	$CH^+ + H_2CO \rightarrow H_3CO^+ + C$	$k_{262} = 9.60 \times 10^{-10}$	M97
263	$CH^+ + O_2 \rightarrow HCO^+ + O$	$k_{263} = 9.70 \times 10^{-10}$	M97
264	$CH^+ + O_2 \rightarrow HCO + O^+$	$k_{264} = 1.00 \times 10^{-11}$	M97
265	$CH^+ + O_2 \rightarrow CO^+ + OH$	$k_{265} = 1.00 \times 10^{-11}$	M97
266	$CH^+ + CO_2 \rightarrow HCO^+ + CO$	$k_{266} = 1.60 \times 10^{-9}$	M97
267	$CH_2^+ + O \rightarrow HCO^+ + H$	$k_{267} = 7.50 \times 10^{-10}$	M97
268	$CH_2^+ + H_2 \rightarrow CH_3^+ + H$	$k_{268} = 1.60 \times 10^{-9}$	M97
269	$CH_2^+ + H_2O \rightarrow H_3CO^+ + H$	$k_{269} = 1.20 \times 10^{-9}$	M97
270	$CH_2^+ + HCO \rightarrow CH_3^+ + CO$	$k_{270} = 4.50 \times 10^{-10}$	M97
271	$CH_2^+ + H_2CO \rightarrow HCO^+ + CH_3$	$k_{271} = 2.81 \times 10^{-9}$	M97

Table 1—Continued

Number	Reaction	Rate Coefficient [a]	Reference [b]
272	$CH_2^+ + O_2 \rightarrow HCO^+ + OH$	$k_{272} = 9.10 \times 10^{-10}$	M97
273	$CH_2^+ + CO_2 \rightarrow H_2CO^+ + CO$	$k_{273} = 1.60 \times 10^{-9}$	M97
274	$CH_3^+ + O \rightarrow HCO^+ + H_2$	$k_{274} = 4.00 \times 10^{-10}$	M97
275	$CH_3^+ + O \rightarrow H_2CO^+ + H$	$k_{275} = 4.00 \times 10^{-11}$	M97
276	$CH_3^+ + H_2 \rightarrow CH5^+ + \gamma$	$k_{276} = 1.30 \times 10^{-14}(T/300)^{-1}$	M97
277	$CH_3^+ + OH \rightarrow H_2CO^+ + H_2$	$k_{277} = 7.20 \times 10^{-10}$	M97
278	$CH_3^+ + HCO \rightarrow CH_4^+ + CO$	$k_{278} = 4.40 \times 10^{-10}$	M97
279	$CH_3^+ + HCO \rightarrow HCO^+ + CH_3$	$k_{279} = 4.40 \times 10^{-10}$	M97
280	$CH_3^+ + H_2CO \rightarrow HCO^+ + CH_4$	$k_{280} = 1.60 \times 10^{-9}$	M97
281	$CH_3^+ + O_2 \rightarrow H_3CO^+ + O$	$k_{281} = 5.00 \times 10^{-12}$	M97
282	$O^+ + H \rightarrow H^+ + O$	$k_{282} = 6.80 \times 10^{-10}$	M97
283	$O^+ + H^- \rightarrow H + O$	$k_{283} = 2.30 \times 10^{-7}(T/300)^{-0.50}$	M97
284	$O^+ + H_2 \rightarrow OH^+ + H$	$k_{284} = 1.70 \times 10^{-9}$	M97
285	$O^+ + CH \rightarrow CH^+ + O$	$k_{285} = 3.50 \times 10^{-10}$	M97
286	$O^+ + CH \rightarrow CO^+ + H$	$k_{286} = 3.50 \times 10^{-10}$	M97
287	$O^+ + CH_2 \rightarrow CH_2^+ + O$	$k_{287} = 9.70 \times 10^{-10}$	M97
288	$O^+ + CH_4 \rightarrow CH_3^+ + OH$	$k_{288} = 1.10 \times 10^{-10}$	M97
289	$O^+ + CH_4 \rightarrow CH_4^+ + O$	$k_{289} = 8.90 \times 10^{-10}$	M97
290	$O^+ + OH \rightarrow OH^+ + O$	$k_{290} = 3.60 \times 10^{-10}$	M97
291	$O^+ + OH \rightarrow O_2^+ + H$	$k_{291} = 3.60 \times 10^{-10}$	M97
292	$O^+ + H_2O \rightarrow H_2O^+ + O$	$k_{292} = 3.20 \times 10^{-9}$	M97
293	$O^+ + C_2 \rightarrow C_2^+ + O$	$k_{293} = 4.80 \times 10^{-10}$	M97
294	$O^+ + C_2 \rightarrow CO^+ + C$	$k_{294} = 4.80 \times 10^{-10}$	M97
295	$O^+ + HCO \rightarrow OH^+ + CO$	$k_{295} = 4.30 \times 10^{-10}$	M97
296	$O^+ + HCO \rightarrow HCO^+ + O$	$k_{296} = 4.30 \times 10^{-10}$	M97
297	$O^+ + H_2CO \rightarrow HCO^+ + OH$	$k_{297} = 1.40 \times 10^{-9}$	M97
298	$O^+ + H_2CO \rightarrow H_2CO^+ + O$	$k_{298} = 2.10 \times 10^{-9}$	M97
299	$O^+ + O_2 \rightarrow O_2^+ + O$	$k_{299} = 1.90 \times 10^{-11}$	M97
300	$O^+ + CO_2 \rightarrow O_2^+ + CO$	$k_{300} = 9.40 \times 10^{-10}$	M97
301	$CH_4^+ + H \rightarrow CH_3^+ + H_2$	$k_{301} = 1.00 \times 10^{-11}$	M97
302	$CH_4^+ + O \rightarrow CH_3^+ + OH$	$k_{302} = 1.00 \times 10^{-9}$	M97
303	$CH_4^+ + H_2 \rightarrow CH5^+ + H$	$k_{303} = 3.30 \times 10^{-11}$	M97
304	$CH_4^+ + CH_4 \rightarrow CH5^+ + CH_3$	$k_{304} = 1.50 \times 10^{-9}$	M97
305	$CH_4^+ + H_2O \rightarrow H_3O^+ + CH_3$	$k_{305} = 2.60 \times 10^{-9}$	M97
306	$CH_4^+ + CO \rightarrow HCO^+ + CH_3$	$k_{306} = 1.40 \times 10^{-9}$	M97
307	$CH_4^+ + H_2CO \rightarrow H_2CO^+ + CH_4$	$k_{307} = 1.62 \times 10^{-9}$	M97
308	$CH_4^+ + H_2CO \rightarrow H_3CO^+ + CH_3$	$k_{308} = 1.98 \times 10^{-9}$	M97
309	$CH_4^+ + O_2 \rightarrow O_2^+ + CH_4$	$k_{309} = 4.00 \times 10^{-10}$	M97
310	$CH_4^+ + CO_2 \rightarrow HCO_2^+ + CH_3$	$k_{310} = 1.20 \times 10^{-9}$	M97
311	$OH^+ + C \rightarrow CH^+ + O$	$k_{311} = 1.20 \times 10^{-9}$	M97
312	$OH^+ + O \rightarrow O_2^+ + H$	$k_{312} = 7.10 \times 10^{-10}$	M97

Table 1—Continued

Number	Reaction	Rate Coefficient [a]	Reference [b]
313	$OH^+ + H_2 \rightarrow H_2O^+ + H$	$k_{313} = 1.01 \times 10^{-9}$	M97
314	$OH^+ + CH \rightarrow CH^+ + OH$	$k_{314} = 3.50 \times 10^{-10}$	M97
315	$OH^+ + CH \rightarrow CH_2^+ + O$	$k_{315} = 3.50 \times 10^{-10}$	M97
316	$OH^+ + CH_2 \rightarrow CH_2^+ + OH$	$k_{316} = 4.80 \times 10^{-10}$	M97
317	$OH^+ + CH_2 \rightarrow CH_3^+ + O$	$k_{317} = 4.80 \times 10^{-10}$	M97
318	$OH^+ + CH_4 \rightarrow H_3O^+ + CH_2$	$k_{318} = 1.31 \times 10^{-9}$	M97
319	$OH^+ + CH_4 \rightarrow CH5^+ + O$	$k_{319} = 1.95 \times 10^{-10}$	M97
320	$OH^+ + OH \rightarrow H_2O^+ + O$	$k_{320} = 7.00 \times 10^{-10}$	M97
321	$OH^+ + H_2O \rightarrow H_2O^+ + OH$	$k_{321} = 1.59 \times 10^{-9}$	M97
322	$OH^+ + H_2O \rightarrow H_3O^+ + O$	$k_{322} = 1.30 \times 10^{-9}$	M97
323	$OH^+ + C_2 \rightarrow C_2^+ + OH$	$k_{323} = 4.80 \times 10^{-10}$	M97
324	$OH^+ + CO \rightarrow HCO^+ + O$	$k_{324} = 1.05 \times 10^{-9}$	M97
325	$OH^+ + HCO \rightarrow H_2O^+ + CO$	$k_{325} = 2.80 \times 10^{-10}$	M97
326	$OH^+ + HCO \rightarrow HCO^+ + OH$	$k_{326} = 2.80 \times 10^{-10}$	M97
327	$OH^+ + HCO \rightarrow H_2CO^+ + O$	$k_{327} = 2.80 \times 10^{-10}$	M97
328	$OH^+ + H_2CO \rightarrow H_3CO^+ + O$	$k_{328} = 1.12 \times 10^{-9}$	M97
329	$OH^+ + H_2CO \rightarrow H_2CO^+ + OH$	$k_{329} = 7.44 \times 10^{-10}$	M97
330	$OH^+ + O_2 \rightarrow O_2^+ + OH$	$k_{330} = 5.90 \times 10^{-10}$	M97
331	$OH^+ + CO_2 \rightarrow HCO_2^+ + O$	$k_{331} = 1.44 \times 10^{-9}$	M97
332	$CH5^+ + H \rightarrow CH_4^+ + H_2$	$k_{332} = 2.00 \times 10^{-11}$	M97
333	$CH5^+ + C \rightarrow CH^+ + CH_4$	$k_{333} = 1.20 \times 10^{-9}$	M97
334	$CH5^+ + O \rightarrow H_3O^+ + CH_2$	$k_{334} = 2.20 \times 10^{-10}$	M97
335	$CH5^+ + O \rightarrow H_3CO^+ + H_2$	$k_{335} = 4.40 \times 10^{-12}$	M97
336	$CH5^+ + CH \rightarrow CH_2^+ + CH_4$	$k_{336} = 6.90 \times 10^{-10}$	M97
337	$CH5^+ + CH_2 \rightarrow CH_3^+ + CH_4$	$k_{337} = 9.60 \times 10^{-10}$	M97
338	$CH5^+ + OH \rightarrow H_2O^+ + CH_4$	$k_{338} = 7.00 \times 10^{-10}$	M97
339	$CH5^+ + H_2O \rightarrow H_3O^+ + CH_4$	$k_{339} = 3.70 \times 10^{-9}$	M97
340	$CH5^+ + CO \rightarrow HCO^+ + CH_4$	$k_{340} = 1.00 \times 10^{-9}$	M97
341	$CH5^+ + HCO \rightarrow H_2CO^+ + CH_4$	$k_{341} = 8.50 \times 10^{-10}$	M97
342	$CH5^+ + H_2CO \rightarrow H_3CO^+ + CH_4$	$k_{342} = 4.50 \times 10^{-9}$	M97
343	$CH5^+ + CO_2 \rightarrow HCO_2^+ + CH_4$	$k_{343} = 3.20 \times 10^{-11}$	M97
344	$H_2O^+ + C \rightarrow CH^+ + OH$	$k_{344} = 1.10 \times 10^{-9}$	M97
345	$H_2O^+ + O \rightarrow O_2^+ + H_2$	$k_{345} = 4.00 \times 10^{-11}$	M97
346	$H_2O^+ + H_2 \rightarrow H_3O^+ + H$	$k_{346} = 8.30 \times 10^{-10}$	M97
347	$H_2O^+ + CH \rightarrow CH^+ + H_2O$	$k_{347} = 3.40 \times 10^{-10}$	M97
348	$H_2O^+ + CH \rightarrow CH_2^+ + OH$	$k_{348} = 3.40 \times 10^{-10}$	M97
349	$H_2O^+ + CH_2 \rightarrow CH_3^+ + OH$	$k_{349} = 4.70 \times 10^{-10}$	M97
350	$H_2O^+ + CH_2 \rightarrow CH_2^+ + H_2O$	$k_{350} = 4.70 \times 10^{-10}$	M97
351	$H_2O^+ + CH_4 \rightarrow H_3O^+ + CH_3$	$k_{351} = 1.11 \times 10^{-9}$	M97
352	$H_2O^+ + OH \rightarrow H_3O^+ + O$	$k_{352} = 6.90 \times 10^{-10}$	M97
353	$H_2O^+ + H_2O \rightarrow H_3O^+ + OH$	$k_{353} = 2.10 \times 10^{-9}$	M97

Table 1—Continued

Number	Reaction	Rate Coefficient [a]	Reference [b]
354	$H_2O^+ + C_2 \rightarrow C_2^+ + H_2O$	$k_{354} = 4.70 \times 10^{-10}$	M97
355	$H_2O^+ + CO \rightarrow HCO^+ + OH$	$k_{355} = 5.00 \times 10^{-10}$	M97
356	$H_2O^+ + HCO \rightarrow H_3O^+ + CO$	$k_{356} = 2.80 \times 10^{-10}$	M97
357	$H_2O^+ + HCO \rightarrow HCO^+ + H_2O$	$k_{357} = 2.80 \times 10^{-10}$	M97
358	$H_2O^+ + HCO \rightarrow H_2CO^+ + OH$	$k_{358} = 2.80 \times 10^{-10}$	M97
359	$H_2O^+ + H_2CO \rightarrow H_2CO^+ + H_2O$	$k_{359} = 1.41 \times 10^{-9}$	M97
360	$H_2O^+ + H_2CO \rightarrow H_3CO^+ + OH$	$k_{360} = 6.62 \times 10^{-10}$	M97
361	$H_2O^+ + O_2 \rightarrow O_2^+ + H_2O$	$k_{361} = 4.30 \times 10^{-10}$	M97
362	$H_3O^+ + C \rightarrow HCO^+ + H_2$	$k_{362} = 1.00 \times 10^{-11}$	M97
363	$H_3O^+ + H^- \rightarrow OH + H_2 + H$	$k_{363} = 2.30 \times 10^{-7}(T/300)^{-0.50}$	M97
364	$H_3O^+ + H^- \rightarrow H_2O + H_2$	$k_{364} = 2.30 \times 10^{-7}(T/300)^{-0.50}$	M97
365	$H_3O^+ + CH \rightarrow CH_2^+ + H_2O$	$k_{365} = 6.80 \times 10^{-10}$	M97
366	$H_3O^+ + CH_2 \rightarrow CH_3^+ + H_2O$	$k_{366} = 9.40 \times 10^{-10}$	M97
367	$H_3O^+ + H_2CO \rightarrow H_3CO^+ + H_2O$	$k_{367} = 3.40 \times 10^{-9}$	M97
368	$C_2^+ + C \rightarrow C^+ + C_2$	$k_{368} = 1.10 \times 10^{-10}$	M97
369	$C_2^+ + O \rightarrow CO^+ + C$	$k_{369} = 3.10 \times 10^{-10}$	M97
370	$C_2^+ + CH \rightarrow CH^+ + C_2$	$k_{370} = 3.20 \times 10^{-10}$	M97
371	$C_2^+ + CH_2 \rightarrow CH_2^+ + C_2$	$k_{371} = 4.50 \times 10^{-10}$	M97
372	$C_2^+ + OH \rightarrow OH^+ + C_2$	$k_{372} = 6.50 \times 10^{-10}$	M97
373	$C_2^+ + HCO \rightarrow HCO^+ + C_2$	$k_{373} = 3.80 \times 10^{-10}$	M97
374	$C_2^+ + O_2 \rightarrow CO^+ + CO$	$k_{374} = 8.00 \times 10^{-10}$	M97
375	$CO^+ + H \rightarrow H^+ + CO$	$k_{375} = 7.50 \times 10^{-10}$	M97
376	$CO^+ + C \rightarrow C^+ + CO$	$k_{376} = 1.10 \times 10^{-10}$	M97
377	$CO^+ + O \rightarrow O^+ + CO$	$k_{377} = 1.40 \times 10^{-10}$	M97
378	$CO^+ + H_2 \rightarrow HCO^+ + H$	$k_{378} = 1.80 \times 10^{-9}$	M97
379	$CO^+ + CH \rightarrow CH^+ + CO$	$k_{379} = 3.20 \times 10^{-10}$	M97
380	$CO^+ + CH \rightarrow HCO^+ + C$	$k_{380} = 3.20 \times 10^{-10}$	M97
381	$CO^+ + CH_2 \rightarrow CH_2^+ + CO$	$k_{381} = 4.30 \times 10^{-10}$	M97
382	$CO^+ + CH_2 \rightarrow HCO^+ + CH$	$k_{382} = 4.30 \times 10^{-10}$	M97
383	$CO^+ + CH_4 \rightarrow CH_4^+ + CO$	$k_{383} = 7.93 \times 10^{-10}$	M97
384	$CO^+ + CH_4 \rightarrow HCO^+ + CH_3$	$k_{384} = 4.55 \times 10^{-10}$	M97
385	$CO^+ + OH \rightarrow OH^+ + CO$	$k_{385} = 3.10 \times 10^{-10}$	M97
386	$CO^+ + OH \rightarrow HCO^+ + O$	$k_{386} = 3.10 \times 10^{-10}$	M97
387	$CO^+ + H_2O \rightarrow H_2O^+ + CO$	$k_{387} = 1.72 \times 10^{-9}$	M97
388	$CO^+ + H_2O \rightarrow HCO^+ + OH$	$k_{388} = 8.84 \times 10^{-10}$	M97
389	$CO^+ + C_2 \rightarrow C_2^+ + CO$	$k_{389} = 8.40 \times 10^{-10}$	M97
390	$CO^+ + HCO \rightarrow HCO^+ + CO$	$k_{390} = 7.40 \times 10^{-10}$	M97
391	$CO^+ + H_2CO \rightarrow HCO^+ + HCO$	$k_{391} = 1.65 \times 10^{-9}$	M97
392	$CO^+ + H_2CO \rightarrow H_2CO^+ + CO$	$k_{392} = 1.35 \times 10^{-9}$	M97
393	$CO^+ + O_2 \rightarrow O_2^+ + CO$	$k_{393} = 1.20 \times 10^{-10}$	M97
394	$HCO^+ + C \rightarrow CH^+ + CO$	$k_{394} = 1.10 \times 10^{-9}$	M97

Table 1—Continued

Number	Reaction	Rate Coefficient [a]	Reference [b]
395	$HCO^+ + H^- \rightarrow CO + H_2$	$k_{395} = 2.30 \times 10^{-7}(T/300)^{-0.50}$	M97
396	$HCO^+ + CH \rightarrow CH_2^+ + CO$	$k_{396} = 6.30 \times 10^{-10}$	M97
397	$HCO^+ + CH_2 \rightarrow CH_3^+ + CO$	$k_{397} = 8.60 \times 10^{-10}$	M97
398	$HCO^+ + OH \rightarrow H_2O^+ + CO$	$k_{398} = 6.20 \times 10^{-10}$	M97
399	$HCO^+ + OH \rightarrow HCO_2^+ + H$	$k_{399} = 1.00 \times 10^{-9}$	M97
400	$HCO^+ + H_2O \rightarrow H_3O^+ + CO$	$k_{400} = 2.50 \times 10^{-9}$	M97
401	$HCO^+ + HCO \rightarrow H_2CO^+ + CO$	$k_{401} = 7.30 \times 10^{-10}$	M97
402	$HCO^+ + H_2CO \rightarrow H_3CO^+ + CO$	$k_{402} = 3.30 \times 10^{-9}$	M97
403	$H_2CO^+ + CH \rightarrow CH^+ + H_2CO$	$k_{403} = 3.10 \times 10^{-10}$	M97
404	$H_2CO^+ + CH \rightarrow CH_2^+ + HCO$	$k_{404} = 3.10 \times 10^{-10}$	M97
405	$H_2CO^+ + CH_2 \rightarrow CH_3^+ + HCO$	$k_{405} = 4.30 \times 10^{-10}$	M97
406	$H_2CO^+ + CH_2 \rightarrow CH_2^+ + H_2CO$	$k_{406} = 4.30 \times 10^{-10}$	M97
407	$H_2CO^+ + CH_4 \rightarrow H_3CO^+ + CH_3$	$k_{407} = 9.35 \times 10^{-11}$	M97
408	$H_2CO^+ + H_2O \rightarrow H_3O^+ + HCO$	$k_{408} = 2.60 \times 10^{-9}$	M97
409	$H_2CO^+ + HCO \rightarrow HCO^+ + H_2CO$	$k_{409} = 3.60 \times 10^{-10}$	M97
410	$H_2CO^+ + HCO \rightarrow H_3CO^+ + CO$	$k_{410} = 3.60 \times 10^{-10}$	M97
411	$H_2CO^+ + H_2CO \rightarrow H_3CO^+ + HCO$	$k_{411} = 3.20 \times 10^{-9}$	M97
412	$H_2CO^+ + O_2 \rightarrow HCO^+ + O_2H$	$k_{412} = 7.70 \times 10^{-11}$	M97
413	$H_3CO^+ + CH \rightarrow CH_2^+ + H_2CO$	$k_{413} = 6.20 \times 10^{-10}$	M97
414	$H_3CO^+ + H_2O \rightarrow H_3O^+ + H_2CO$	$k_{414} = 2.30 \times 10^{-10}$	M97
415	$O_2^+ + C \rightarrow CO^+ + O$	$k_{415} = 5.20 \times 10^{-11}$	M97
416	$O_2^+ + C \rightarrow C^+ + O_2$	$k_{416} = 5.20 \times 10^{-11}$	M97
417	$O_2^+ + CH \rightarrow CH^+ + O_2$	$k_{417} = 3.10 \times 10^{-10}$	M97
418	$O_2^+ + CH \rightarrow HCO^+ + O$	$k_{418} = 3.10 \times 10^{-10}$	M97
419	$O_2^+ + CH_2 \rightarrow H_2CO^+ + O$	$k_{419} = 4.30 \times 10^{-10}$	M97
420	$O_2^+ + CH_2 \rightarrow CH_2^+ + O_2$	$k_{420} = 4.30 \times 10^{-10}$	M97
421	$O_2^+ + C_2 \rightarrow CO^+ + CO$	$k_{421} = 4.10 \times 10^{-10}$	M97
422	$O_2^+ + C_2 \rightarrow C_2^+ + O_2$	$k_{422} = 4.10 \times 10^{-10}$	M97
423	$O_2^+ + HCO \rightarrow O_2H^+ + CO$	$k_{423} = 3.60 \times 10^{-10}$	M97
424	$O_2^+ + HCO \rightarrow HCO^+ + O_2$	$k_{424} = 3.60 \times 10^{-10}$	M97
425	$O_2^+ + H_2CO \rightarrow HCO^+ + O_2 + H$	$k_{425} = 2.30 \times 10^{-10}$	M97
426	$O_2^+ + H_2CO \rightarrow H_2CO^+ + O_2$	$k_{426} = 2.07 \times 10^{-9}$	M97
427	$O_2H^+ + C \rightarrow CH^+ + O_2$	$k_{427} = 1.00 \times 10^{-9}$	M97
428	$O_2H^+ + O \rightarrow OH^+ + O_2$	$k_{428} = 6.20 \times 10^{-10}$	M97
429	$O_2H^+ + H_2 \rightarrow H_3^+ + O_2$	$k_{429} = 6.40 \times 10^{-10}$	M97
430	$O_2H^+ + CH \rightarrow CH_2^+ + O_2$	$k_{430} = 6.20 \times 10^{-10}$	M97
431	$O_2H^+ + CH_2 \rightarrow CH_3^+ + O_2$	$k_{431} = 8.50 \times 10^{-10}$	M97
432	$O_2H^+ + OH \rightarrow H_2O^+ + O_2$	$k_{432} = 6.10 \times 10^{-10}$	M97
433	$O_2H^+ + H_2O \rightarrow H_3O^+ + O_2$	$k_{433} = 8.20 \times 10^{-10}$	M97
434	$O_2H^+ + CO \rightarrow HCO^+ + O_2$	$k_{434} = 8.40 \times 10^{-10}$	M97
435	$O_2H^+ + HCO \rightarrow H_2CO^+ + O_2$	$k_{435} = 7.10 \times 10^{-10}$	M97

Table 1—Continued

Number	Reaction	Rate Coefficient [a]	Reference [b]
436	$O_2H^+ + H_2CO \rightarrow H_3CO^+ + O_2$	$k_{436} = 9.80 \times 10^{-10}$	M97
437	$O_2H^+ + CO_2 \rightarrow HCO_2^+ + O_2$	$k_{437} = 1.10 \times 10^{-9}$	M97
438	$HCO_2^+ + C \rightarrow CH^+ + CO_2$	$k_{438} = 1.00 \times 10^{-9}$	M97
439	$HCO_2^+ + O \rightarrow HCO^+ + O_2$	$k_{439} = 1.00 \times 10^{-9}$	M97
440	$HCO_2^+ + CH_4 \rightarrow CH5^+ + CO_2$	$k_{440} = 7.80 \times 10^{-10}$	M97
441	$HCO_2^+ + H_2O \rightarrow H_3O^+ + CO_2$	$k_{441} = 2.30 \times 10^{-9}$	M97
442	$HCO_2^+ + CO \rightarrow HCO^+ + CO_2$	$k_{442} = 7.80 \times 10^{-10}$	M97
443	$C^+ + e \rightarrow C + \gamma$	$k_{443} = 4.40 \times 10^{-12}(T/300)^{-0.61}$	M97
444	$CH^+ + e \rightarrow C + H$	$k_{444} = 1.50 \times 10^{-7}(T/300)^{-0.42}$	M97
445	$CH_2^+ + e \rightarrow C + H_2$	$k_{445} = 1.25 \times 10^{-7}(T/300)^{-0.50}$	M97
446	$CH_2^+ + e \rightarrow CH + H$	$k_{446} = 1.25 \times 10^{-7}(T/300)^{-0.50}$	M97
447	$CH_3^+ + e \rightarrow CH_2 + H$	$k_{447} = 7.75 \times 10^{-8}(T/300)^{-0.50}$	M97
448	$CH_3^+ + e \rightarrow CH + H_2$	$k_{448} = 1.95 \times 10^{-7}(T/300)^{-0.50}$	M97
449	$CH_3^+ + e \rightarrow CH + 2H$	$k_{449} = 7.75 \times 10^{-8}(T/300)^{-0.50}$	M97
450	$CH_3^+ + e \rightarrow CH_3 + \gamma$	$k_{450} = 1.10 \times 10^{-10}(T/300)^{-0.50}$	M97
451	$O^+ + e \rightarrow O + \gamma$	$k_{451} = 3.40 \times 10^{-12}(T/300)^{-0.63}$	M97
452	$CH_4^+ + e \rightarrow CH_3 + H$	$k_{452} = 1.75 \times 10^{-7}(T/300)^{-0.50}$	M97
453	$CH_4^+ + e \rightarrow CH_2 + 2H$	$k_{453} = 1.75 \times 10^{-7}(T/300)^{-0.50}$	M97
454	$OH^+ + e \rightarrow O + H$	$k_{454} = 3.75 \times 10^{-8}(T/300)^{-0.50}$	M97
455	$CH5^+ + e \rightarrow CH_4 + H$	$k_{455} = 5.50 \times 10^{-7}(T/300)^{-0.30}$	M97
456	$CH5^+ + e \rightarrow CH_3 + H_2$	$k_{456} = 5.50 \times 10^{-7}(T/300)^{-0.30}$	M97
457	$H_2O^+ + e \rightarrow OH + H$	$k_{457} = 1.60 \times 10^{-7}(T/300)^{-0.50}$	M97
458	$H_2O^+ + e \rightarrow O + H_2$	$k_{458} = 2.00 \times 10^{-7}(T/300)^{-0.50}$	M97
459	$H_3O^+ + e \rightarrow H_2O + H$	$k_{459} = 3.50 \times 10^{-7}(T/300)^{-0.50}$	M97
460	$H_3O^+ + e \rightarrow OH + 2H$	$k_{460} = 6.50 \times 10^{-7}(T/300)^{-0.50}$	M97
461	$C_2^+ + e \rightarrow 2C$	$k_{461} = 3.00 \times 10^{-7}(T/300)^{-0.50}$	M97
462	$CO^+ + e \rightarrow O + C$	$k_{462} = 1.80 \times 10^{-7}(T/300)^{-0.50}$	M97
463	$HCO^+ + e \rightarrow CO + H$	$k_{463} = 1.10 \times 10^{-7}(T/300)^{-1.00}$	M97
464	$H_2CO^+ + e \rightarrow HCO + H$	$k_{464} = 1.00 \times 10^{-7}(T/300)^{-0.50}$	M97
465	$H_2CO^+ + e \rightarrow CO + 2H$	$k_{465} = 5.00 \times 10^{-7}(T/300)^{-0.50}$	M97
466	$H_2CO^+ + e \rightarrow H_2CO + \gamma$	$k_{466} = 1.10 \times 10^{-10}(T/300)^{-0.70}$	M97
467	$H_3CO^+ + e \rightarrow CO + H + H_2$	$k_{467} = 2.00 \times 10^{-7}(T/300)^{-0.50}$	M97
468	$H_3CO^+ + e \rightarrow HCO + 2H$	$k_{468} = 2.00 \times 10^{-7}(T/300)^{-0.50}$	M97
469	$H_3CO^+ + e \rightarrow H_2CO + H$	$k_{469} = 2.00 \times 10^{-7}(T/300)^{-0.50}$	M97
470	$O_2^+ + e \rightarrow 2O$	$k_{470} = 1.95 \times 10^{-7}(T/300)^{-0.70}$	M97
471	$O_2H^+ + e \rightarrow O_2 + H$	$k_{471} = 3.00 \times 10^{-7}(T/300)^{-0.50}$	M97
472	$HCO_2^+ + e \rightarrow CO_2 + H$	$k_{472} = 2.40 \times 10^{-7}(T/300)^{-0.50}$	M97
473	$HCO_2^+ + e \rightarrow CO + OH$	$k_{473} = 1.00 \times 10^{-7}(T/300)^{-0.50}$	M97
474	$OH + CH_3 \rightarrow CH_4 + O$	$k_{474} = 3.22 \times 10^{-14}(T/300)^{2.20}\exp(-2240/T)$	M97
475	$H^+ + H_2CO \rightarrow CO^+ + H_2 + H$	$k_{475} = 1.06 \times 10^{-9}$	M97
476	$He^+ + C \rightarrow C^+ + He$	$k_{476} = 6.30 \times 10^{-15}(T/300)^{0.75}$	M97

REFERENCES

Abel, T., Anninos, P., Zhang, Y., & Norman, M. L. 1997, NewA, 2, 181

Carlberg, R. G. 1981, MNRAS, 197, 1021

Galli, D, & Palla, F. 1998, A&A, 335, 403

Haiman, Z., Thoul, A. A., & Loeb, A. 1996, ApJ, 464, 523

Hayashi, C. 1984, Butsuri, 40, 9

Hayashi, C., & Nakano, T. 1965, Prog. Theor. Phys., 34, 754

Hollenbach, D., & McKee, C. F. 1979, ApJS, 41, 555

Hollenbach, D., & McKee, C. F. 1989, ApJ, 342, 306

Izotov, Yu. I., & Kolesnik, I. G. 1984, Soviet Astr., 28, 15

Lahav, O. 1986, MNRAS, 220, 259

Larson, R. B. 1969, MNRAS, 145, 271

Lenzuni, P., Chernoff, D. F., & Salpeter, E. E. 1991, ApJS, 76, 759

Low, C., & Lynden-Bell, D. 1976, MNRAS, 176, 367

Masunaga, H., Miyama, S. M., & Inutsuka, S. 1998, ApJ, 495, 346

Mathis, J. S., Rumpl, W., & Nordsieck, K. H. 1977, ApJ, 217, 425

Matsuda, T., Sato, H., & Takeda, H. 1969, Prog. Theor. Phys., 42, 219

McKee, C. F., Storey, J. W. V., Watson, D. M., & Green, S. 1982, ApJ, 259, 647

Millar, T. J., Farquhar, P. R. A., & Willacy, K. 1997, A&AS121, 139

Miyama, S. M., Narita, S., & Hayashi, C. 1987b, Prog. Theor. Phys., 78, 1051

——— 1987b, Prog. Theor. Phys., 78, 1273

Nakamura, F., & Umemura, M. 1999, ApJ, 515, 239

Narita, S., Nakano, T., & Hayashi, C. 1970, Prog. Theor. Phys., 43, 942

Neufeld, D. A., Lepp, S., & Melnick, G. J. 1995, ApJS, 100, 132

Table 1—Continued

Number	Reaction	Rate Coefficient [a]	Reference [b]
477	$He^+ + H_2CO \rightarrow H_2CO^+ + He$	$k_{477} = 9.69 \times 10^{-10}$	M97
478	$He^+ + H_2CO \rightarrow CH_2^+ + O + He$	$k_{478} = 1.71 \times 10^{-9}$	M97

[a]The temperasture T is in K, except otherwise noted.

[b]A97; Abel et al. (1997), GP98; Galli & Palla (1998), SK87; Shapiro & Kang (1987), M97; Millar et al. (1997), PSS83; Palla et al. (1983), TH85; Tielens & Hollenbach (1985)

Oliveira, S., Miranda, O. D., de Araujo, J. C. N., & Opher, R. 1998, MNRAS, 101, 114

Omukai, K., & Nishi, R. 1998, ApJ, 508, 141

Padmanabhan, T. 1993, Structure Formation in the Universe (Cambridge: Cambridge University Press)

Palla, F., Salpeter, E. E., & Stahler, S. W. 1983, ApJ, 271, 632

Penston, M. V. 1969, MNRAS, 144, 425

Pollack, J. B., Hollenbach, D., Beckwith, S., Simonelli, D. P., Roush, T., & Fong, W. 1994, ApJ, 421, 615

Puy, D., & Signore, M. 1997, NewA, 2, 299

Saslaw, W. C., & Zipoy, D. 1967, Nature, 216, 976

Shapiro, P. R., & Kang, H. 1987, ApJ, 318, 32

Stahler, S. W., Palla, F., & Salpeter, E. E. 1986, ApJ, 302, 590

Stahler, S. W., Shu, F. H., & Taam, R. E. 1980, ApJ, 241, 637

Silk, J. 1977, ApJ, 214, 152

Takahashi, T., Hollenbach, D. J., & Silk, J. 1983, ApJ, 275, 145

Tielens, A. G. G. M., & Hollenbach, D. 1985, ApJ, 291, 722

Tsuribe, T., & Inutsuka, S. 1999, ApJ, 523, L155

Uehara, H., Susa, H., Nishi, R., Yamada, M., & Nakamura, T. 1996, ApJ, 473, L95

Villere, K. R., & Bodenheimer, P. H. 1987, in IAU Symp. 120, Astrochemistry, ed. M. S. Vardya & S. T. Tarafdar (Dordrecht: Reidel), 121

Wolfire, M. G., & Cassinelli, J. P. 1987, ApJ, 319, 850

Yoneyama, T. 1972, PASJ, 24, 87

Yoshii, Y., & Sabano, Y. 1980, PASJ, 32, 229

This preprint was prepared with the AAS LaTeX macros v4.0.

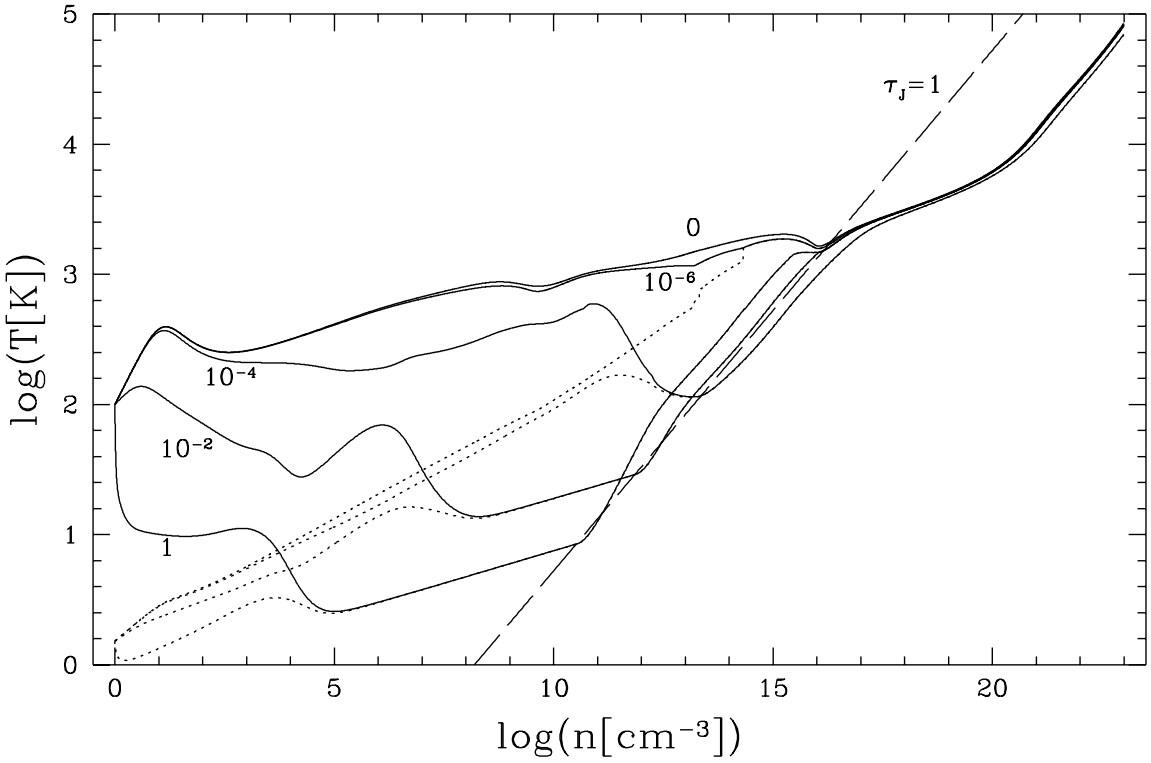

Fig. 1.— The evolutionary trajectories of protostellar clouds with different metallicities. The solid curves show the temperature of the clouds with metallicity (*from the top to bottom*) $z = 0, 10^{-6}, 10^{-4}, 10^{-2}, 1$. The dotted curves show the grain temperature for the same clouds. The initial condition is $T = 100\mathrm{K}, n = 1\mathrm{cm}^{-3}, y(e) = 1 \times 10^{-4}, y(\mathrm{H}_2) = 1 \times 10^{-6}$. Initially, all the carbon is assumed to be in the form of CII, while oxygen is OI. The dashed line marked "$\tau_{\mathrm{J}} = 1$" represents the line L in the text (Eq.35).

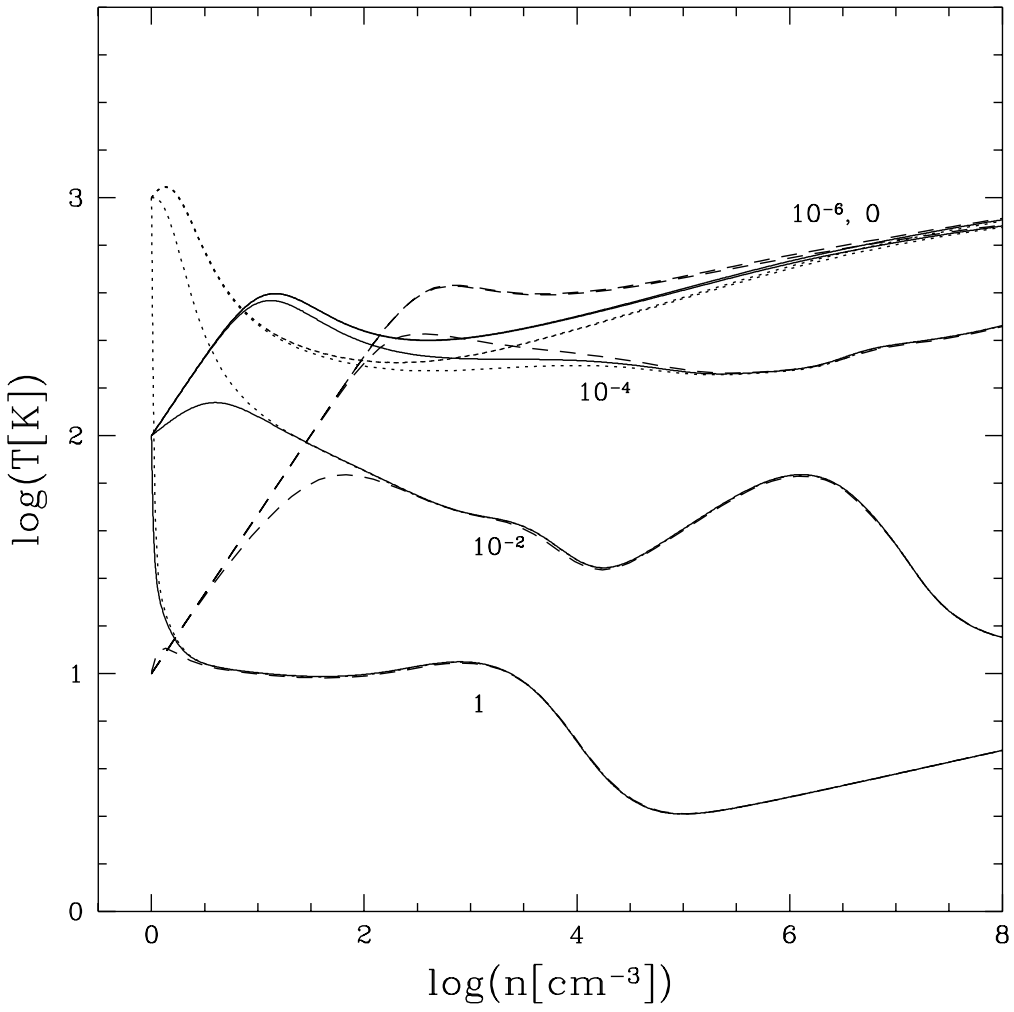

Fig. 2.— Initial condition dependence of the evolutionary trajectories. The solid curves are the same as those of Figure 1 ("fiducial model"). The initial temperature of dotted curves is 1000K and of the dashed curves is 10K, while other quatities are the same as the fiducial model. For same values of metallicity, a wide variation in temperature yields convergent evolutionary tracks.

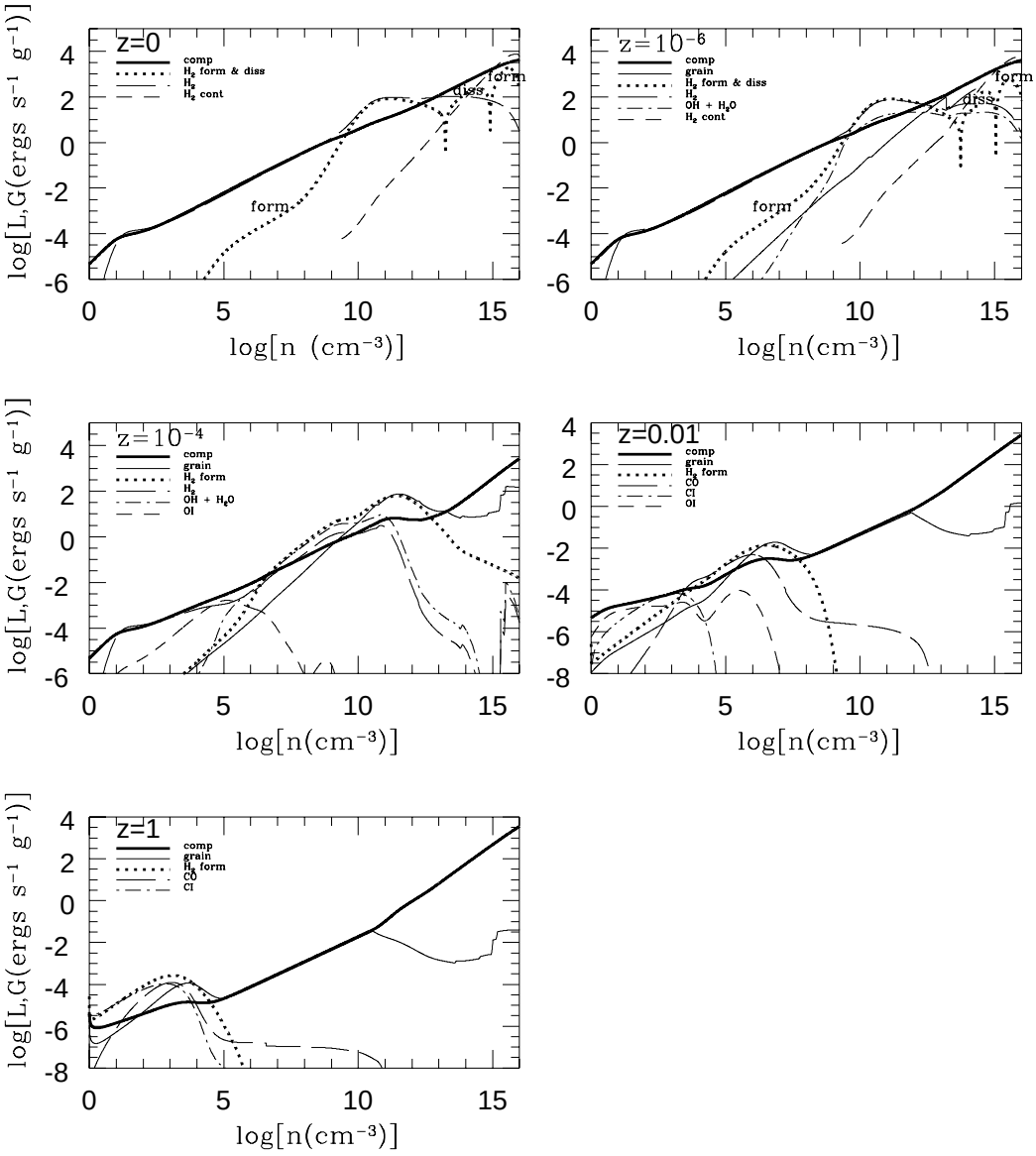

Fig. 3.— The contributions to the cooling/heating rates by major processes for the same clouds as illustrated in Figure 1: (a)$z = 0$, (b)$z = 10^{-6}$, (c)$z = 10^{-4}$, (d)$z = 10^{-2}$, and (e)$z = 1$. Curves labelled "comp", "grain", "H_2 form/diss", and "H_2 cont" show the cooling/heating rate by the adiabatic compression, the gas-grain heat transfer, formation/dissociation of H_2, and H_2 continuum. The other curves labelled "H_2", "OH+H_2O", "CO", "CI", and "OI" illustrate the line cooling rate by these atoms/molecules. Irregularities in "grain" (in panels b-e) and "H_2" and "OH+H_2O"(in panel b and c) cooling rates near $n \sim 10^{14}\mathrm{cm}^{-3}$ are caused by sublimaiton of each grain component and subsequent change of the dust opacity.

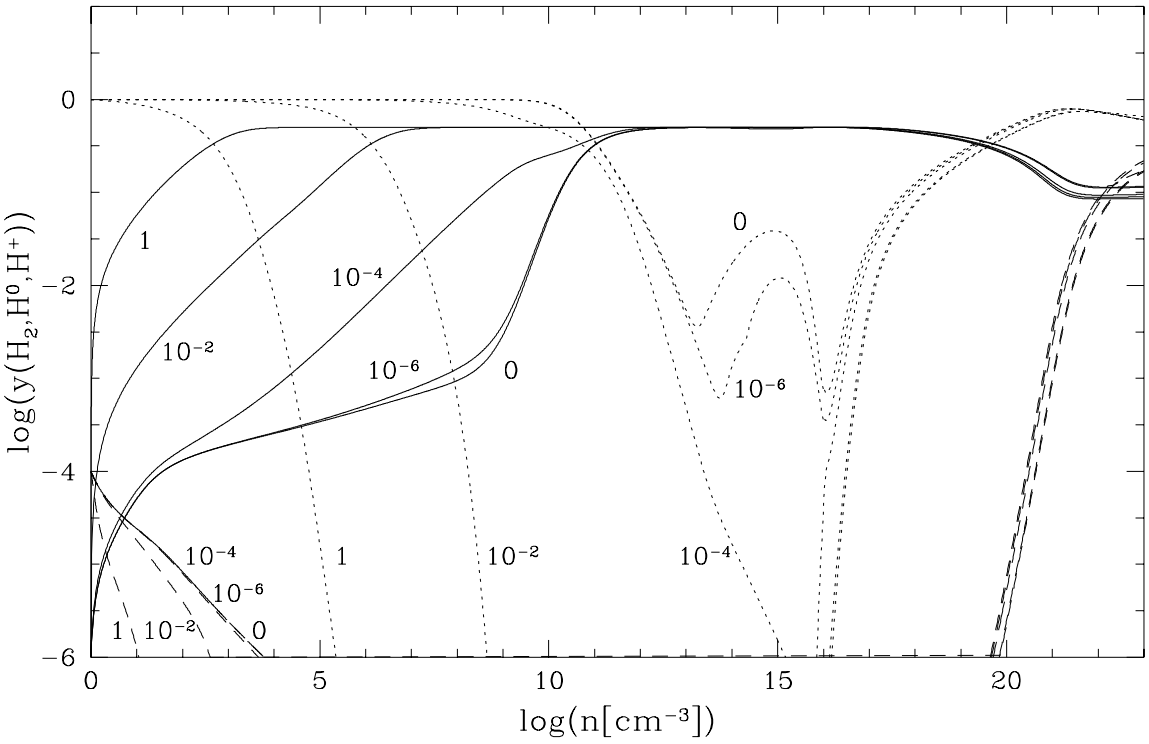

Fig. 4.— The concentrations of hydrogen molecules (*solid line*), atoms (*dotted line*) and ions (*dashed line*) for the same clouds as illustrated in Fig.1.